Universidade de Aveiro
Ano 2017
Departamento de Geociências

Cíntia Marques Pereira

Desafios do *Flex Binning* em Dados de Reflexão Sísmica de Alta Resolução

Challenges in *Flex Binning* Ultra High Resolution Seismic Reflection Data

Universidade de Aveiro
Ano 2017

Departamento de Geociências

Cíntia Marques Pereira

Desafios do *Flex Binning* em Dados de Reflexão Sísmica de Alta Resolução

Challenges in *Flex Binning* Ultra High Resolution Seismic Reflection Data

Dissertação apresentada à Universidade de Aveiro para cumprimento dos requisitos necessários à obtenção do grau de Mestre em Engenharia Geológica, realizada sob a orientação científica do Prof. Doutor Luís Menezes Pinheiro, Professor Associado do Departamento de Geociências da Universidade de Aveiro e do Doutor Henrique Duarte, Director do Departamento de Geofísica Marinha da empresa *Geosurveys*.

O júri

presidente

Prof. Doutor Jorge Manuel Pessoa Girão Medina
Professor Auxiliar do Departamento Geociências da Universidade de Aveiro

Prof. Doutor Luís Filipe Fuentefria de Menezes Pinheiro
Professor Associado do Departamento de Geociências da Universidade de Aveiro

Prof. Doutor Leonardo Azevedo Guerra Raposo Pereira
Professor Auxiliar do Departamento de Engenharia Civil Arquitectura e Georrecursos do Instituto Superior Técnico - Universidade de Lisboa .

Agradecimentos

Quero agradecer aos meus orientadores, o Professor Luís Menezes e ao Doutor Henrique Duarte pela oportunidade que me concederam de puder aprender e trabalhar no âmbito de uma empresa, e pela paciência, apoio, disponibilidade, orientação, conhecimento transmitido e tempo dedicado durante a realização deste trabalho.

Este trabalho não teria sido possível sem as condições que a *Geosurveys* proporcionou para a execução da tese, bem como, a doação das diversas versões do *software Seismic Processing Workshop (SPW)* doado pela *Parallel Geoscience Corporation.*

A todas as pessoas que tive o prazer de conhecer durante o meu estágio na *Geosurveys* e ao meu colega de estágio Fábio Correia, pela boa disposição, pelo ambiente agradável e por todo o auxílio prestado.

Aos meus pais pela oportunidade e por todo o apoio que me deram no decorrer deste percurso.

Ao meu namorado, Elói, por todo o amor, carinho e apoio ao longo deste tempo.

palavras-chave

Flex Binning, reflexão sísmica multi-canal, lacunas em dados de Ultra High Resolution seismic, CMP *Binning*, *Bin* Fold Limit.

resumo

Os dados sísmicos 3D podem conter “lacunas” de cobertura devido a diversos problemas operacionais. As “lacunas” em dados 3D podem causar impactos adversos em várias etapas do processamento de dados, tais como na análise de velocidade, atenuação dos múltiplos, “stack” e migração. O *Flex Binning* é um método expediente para resolver este problema. O método *Flex Binning* permite que cada *bin* contenha mais traços, aumentando o tamanho efectivo de cada *bin* e incluindo traços dos *bins* vizinhos. O desafio é aplicar o *Flex Binning* a um número muito grande de traços que excedem as soluções actuais de *design* de *software* e capacidade de *hardware*. Vários testes foram realizados no *software* Seismic Processing Workshop (SPW). Durante os vários testes realizados, foi possível detectar e resolver problemas de código e “bugs” de *software* tais como, por exemplo, a incapacidade de aplicar uma grelha ao conjunto de dados e deixar traços fora da grelha. A questão da indexação foi outro problema detectado, que se resolveu por uma mudança de *design* do *software* no fluxo de processamento *CMP Binning*. A realização de vários testes nas diversas versões do SPW permitiu avanços na implementação do *Flex Binning* para conjuntos de dados de elevadas dimensões, nomeadamente a execução do fluxo CMP *Binning* com sucesso num conjunto de dados com 751GB. No fluxo de processamento *CMP Binning,* antes destes testes só era possível aplicar o *Flex Binning* corretamente a um conjunto de dados com aproximadamente 30 GB de tamanho.

keywords

Flex Binning, multi-channel seismic reflection, gaps in large UHRS data, CMP *Binning Bin* Fold Limit.

abstract

3D seismic reflection data may contain coverage gaps due to operational problems. The gaps in 3D data can cause adverse impacts in several steps of the data processing such as velocity analysis, multiple attenuation, stacking and migration. *Flex Binning* is an expedient method to solve these gaps. The *Flex Binning* method allows each *bin* to contain more traces, by increasing the effective size of each *bin* and thereby include traces which also fall into neighboring *bins*. The challenge is to apply *Flex Binning* to very large number of traces exceeding current *software* design solutions and *hardware* capability. Several tests were performed with the Seismic Processing Workshop (SPW) *software*. During several tests, coding problems and bugs were detected and corrected, such as the inability to apply a grid to the dataset and leave traces out of the grid. Also, proper indexing was also solved by a change of *software* design in CMP *Binning* code. Beta testing on SPW allowed advances in the implementation of *Flex Binning* to large inputs, namely the execution of the CMP *Binning* flow successfully to a dataset with 751GB. The CMP *Binning* step before the tests could only *Flex Binning* effectively to an input with a size of approximately 30 GB.

Table of Contents

List of Figures

List of Tables

List of abbreviations

2D - Two Dimensions

3D – Three Dimensions

A – Amperes

BP- Before Present

CDP – Common Depth Point

CHAN- Channel number

CMP – Common Mid-Point

DGPS - Differential Global Positioning System

FFID- Field File Identify Document number

FR - Fresnel Zone

GPS – Global Positioning System

GS - *Geosurveys*

HOW01 - Hornsea Offshore Windfarm Project One

Hz – HERTZ

I/O – Input/output

ILine – Inline

J- Joule

ka – kilo annum

kV - kilovolts

m - Meters

MIS - Marine Isotope Stages

ms – Milliseconds

NE – Northeast

NMO- Normal Move Out

NW – northwest

QA – Quality Analysis

QC – Quality Control

RC - Reflection Coefficient

SEG Y – Convention from the society of exploration geophysicist (SEG)

SPW – Seismic Processing Workshop

TWT – two-way time

UHRS - Ultra High Resolution Seismic

UKCS – United Kingdom Continental Shelf

WAZ - Wide-Azimuth

WNW - West North West

WTG – Wind Tur*bin*e Generators

XLine – Crossline

Z – Acoustic impedance

1. Introduction

1.1 Nature and scope of this work

The present dissertation is the result of a curricular internship at *Geosurveys - Geophysical Consultants (GS)*, based in Aveiro (Portugal), for a period of eleven months, within the discipline of Dissertation / Project / Internship of the 2nd year of the Master's Degree in Geological Engineering (2nd cycle) of the University of Aveiro, under the supervision of Dr. Henrique Duarte, Director of the *Geosurveys* Marine Geophysics Department, and Professor Luís Menezes Pinheiro of the Department of Geosciences of the University of Aveiro.

1.2 The *Geosurveys* – Geophysical Consultants

The GS was formed in 1999 from an ambitious project, fundamentally oriented to the Prospecting Geophysics and Earth Sciences. To meet market needs, *Geosurveys* specializes in the areas of Geophysical Prospecting and Geology Onshore, Near-shore & Offshore, in the various fields of it is application, namely water resources, planning and management of projects in geophysics, environmental impact, archeology and patrimony, geotechnics and civil engineering, mining prospecting, and risk of natural catastrophes.

Considering the services provided and in order to effectively manage the resources and employees, *Geosurveys* is divided into three Departments: The Financial Department, led by the General Manager Francisco Sobral; the Department of Marine Geophysics, headed by Senior Geophysicist Henrique Duarte; and the Department of Geophysics on Earth, led by Senior Geophysicist Carlos Grangeia. The position of Executive Director is occupied by the Senior Geophysicist Hélder Hermosilha.

These departments consist of multidisciplinary teams of geophysicists, geologists and geological engineers, distributed between office and field, who work to give a good response to the various needs of the various clients.

1.3 Objectives of this work

During the eleven-month internship at *Geosurveys*, in addition to the academic learning strand and the main goal of the research project, it was intended to obtain a professional experience in a business environment, as well as the familiarization with the way a company operates in the field of Marine Geophysics; these objectives have been fully met.

Throughout this internship, several tasks were developed in the scope of the company's operating methods, in order to get familiar with the daily routines of the workers in a multi-channel seismic reflection data processing workstation, to learn to use processing and geological interpretation *software*, such as *RadEx Pro* (*Deco Geophysical*), *ProMAX* (*Landmark Graphics Corporation*) and *Kingdom Suite* (*IHS Energy*) as well as other industry standard *software*. Some of this knowledge was applied to the case study presented in this thesis.

In order to gain experience and grow on a professional level, participation as a *Trainee* in some of the processing and geological interpretation projects carried out by the company has contributed extensively for this purpose. After an initial period of adjustment, the main activities concentrated on the proposed research work on the challenges of the application of the *Flex Binning* method to large datasets.

3D seismic reflection data may contain coverage gaps due to operational problems. These gaps can cause adverse impacts in several steps of the data processing such as velocity analysis, multiple attenuation, stacking and migration. *Flex Binning* is an expedient method to solve these gaps. This method allows each *bin* to contain more traces, by increasing the effective size of each *bin* and thereby including traces which also fall into neighboring *bins*.

The main objective and challenge of this project is to apply *Flex Binning* to very large number of traces exceeding current *software* design solutions and *hardware* capability. Several tests were performed on the Seismic Processing Workshop *software*. Beta testing on SPW carried out in the scope of this wok allowed significant advances to be made in the implementation of *Flex Binning* and made possible its application to large input datasets.

1.4 Location of the Study Area

The study area is the Hornsea Offshore Windfarm Project One (HOW01), located in the southern North Sea, about 150 km from the Eastern coast of England, Great Britain (Figure 1).

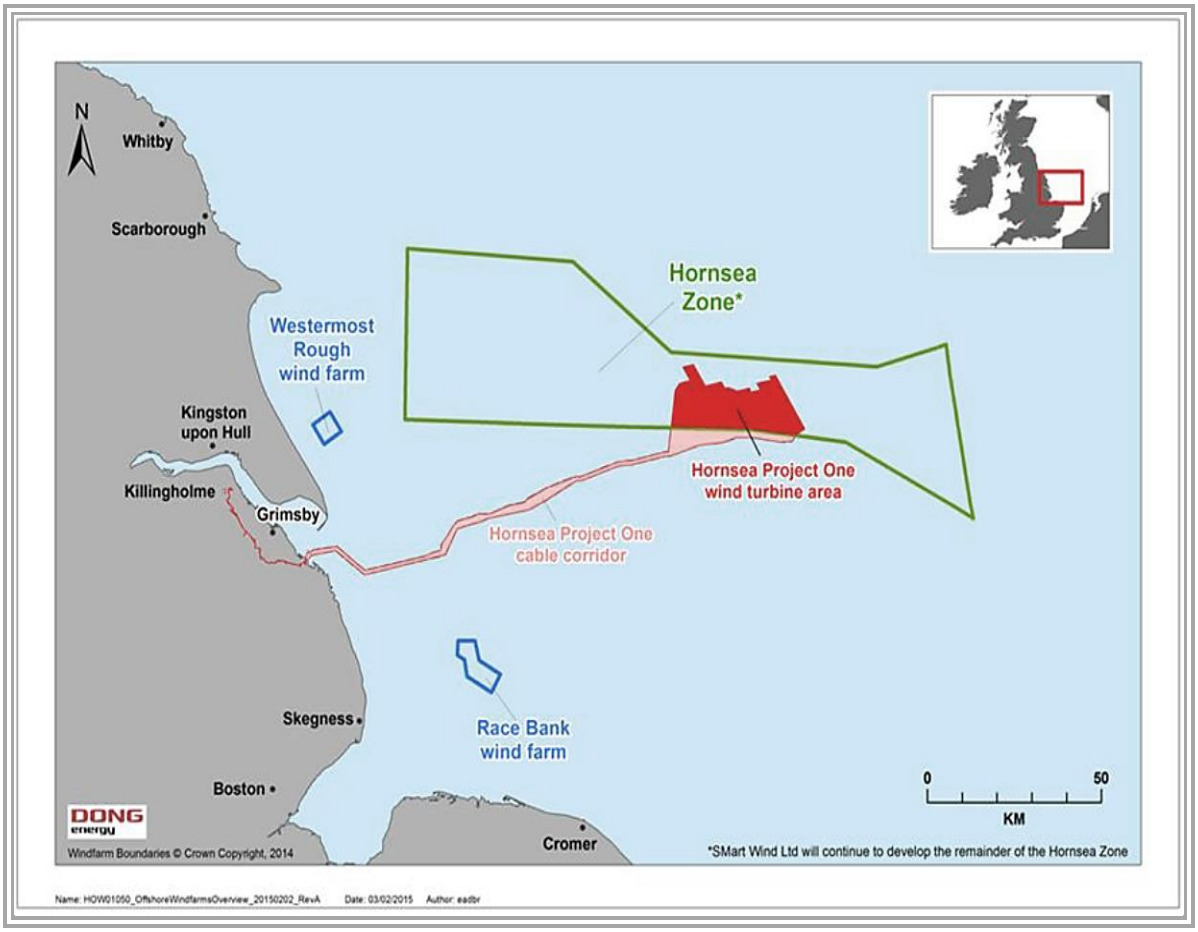

Figure 1. Schematic image the survey area HOW01. Image from Dong Energy.

1.5 Structure of this thesis

This work contains of six chapters, followed by bibliographical references, and is structured as follows:

- Chapter 1: Introduction. This chapter specifies the nature and scope of this work, presents the company *Geosurveys*, defines the general objectives, the location of the study area, and ends with a brief description of the thesis structure.
- Chapter 2: The 3D Ultra High Resolution Seismic Reflection Method. This chapter presents a general introduction to the fundamental principles of the seismic method and the

acquisition of multi-channel reflection seismic; including the acquisition equipment used in the marine environment and finally ends with a brief description of the basic seismic data processing steps.

- Chapter 3: The Hornsea Offshore Windfarm Project One - 3D UHRS Survey – Case Study. This chapter describes the way in which data acquisition was conducted, makes a preliminary interpretation to relate to the geological framework and explains the problems that exist in 3D seismic blocks.
- Chapter 4: *Flex Binning* Implementation in SPW. This chapter explain what is *Flex Binning* method, the *Flex Binning* routines in SPW and the beta testing, the problems encountered and the solutions adopted.
- Chapter 5: Results and Discussion. In this chapter were describe the results obtained with application of *Flex Binning* to a UHRS dataset; comments the results obtained and highlights the progress made in the implementation of *Flex Binning*.
- Chapter 6: Conclusions. This chapter presents a summary of the main results obtained and suggests future work in this line of research.
- Chapter 7: References. In this chapter it was possible see the references which was used as basis for performing this master thesis.

2. The 3D Ultra High Resolution Seismic Reflection Method

2.1 Basic Principles and Fundamentals

The seismic reflection method, consists in emitting seismic waves (or seismic pulses) from at or near surface and record their return to the surface after reflection on the interfaces between the various subsurface formations with different acoustic and physical properties, and measuring the traveltimes and amplitudes, in order to reconstruct the subsurface geology. According to the Snell's Law (Equation 1), the incident wave at an interface between two distinct layers is divided into a refracted part that continues to propagate downward in a slightly different direction than the incident wave and a reflected part that travels back to the surface.

$$\frac{\sin\theta_i}{\sin\theta_r} = \frac{V_1}{V_2} \qquad \text{(Eq.1)}$$

Where θ_i is the incident angle, θ_r is the refracted angle, and V_1 and V_2 represent the velocities of the seismic waves in two different media.

In reality, what happens in the case of the non-normal incidence (Figure 2) is that there is a partition of energy at the interface and there will be wave mode conversion at the interface: shear waves (S-waves) are converted to longitudinal waves (P-waves) and vice-versa (Sheriff and Geldart, 1995; Telford et al., 1990). In order to determine the amplitude of the various reflected and refracted waves at a plane interface for an incident P-wave it is necessary to apply the Zoeppritz equations (Sheriff and Geldart, 1995; Telford et al., 1990).

The P-waves are longitudinal and compressive, and travel at a velocity that depends on the elastic properties and densities of the rocks. The medium particles during S-wave propagation vibrate in a transverse way, with oscillatory movement's perpendicular to the direction of propagation, causing shear when the wave is transmitted, and propagate slower than the P-waves. Another characteristic of the S-waves it is that they cannot propagate in fluids, since these are not capable to suffer shear.

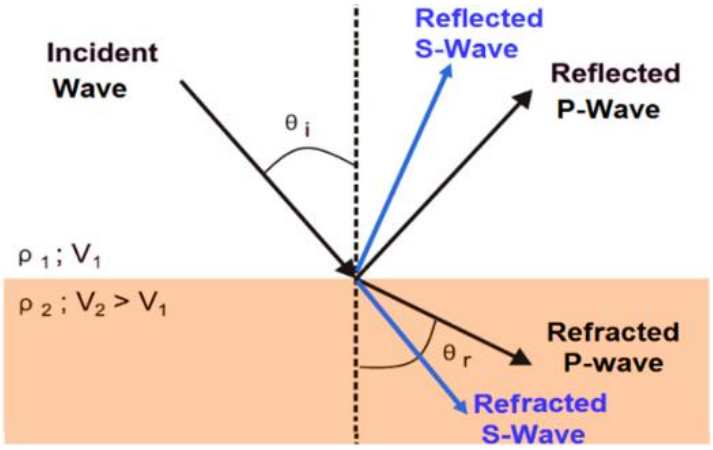

Figure 2. Schematic image of the seismic wave between two media with different physical properties. The non-normal incidence. ρ_1 and ρ_2 represent the density values for the two different layers. V_1 and V_2 represent the velocity values of the seismic waves (adapted from Ribeiro, 2011).

In order to get information about the subsurface geology, as well as the rock properties and layers attitude, the traveltimes and amplitude of the reflected waves from the source through the subsurface and then back to the receivers are recorded, processed and interpreted.

The two-way time (TWT) is the time that a wave takes to travel from its source, down to an interface between two layers with different physical properties (specifically the density (ρ) and the seismic wave velocity (V)) and back to the surface where it is recorded by the receivers. The acoustic impedance (Z) is the product of the density the formation by the velocity of propagation of the waves in that formation.

The difference between the formations with diverse physical proprieties provides us with a contrast of acoustic impedance (Z). The Reflection Coefficient (RC) between two layers, for the simplified case of normal incidence is proportional to the acoustic impedance contrast (Equation 2, valid only for normal incidence).

$$RC = \frac{\rho_2 * V_2 - \rho_1 * V_1}{\rho_2 * V_2 + \rho_1 * V_1} = \frac{Z_2 - Z_1}{Z_2 + Z_1} \qquad \text{(Eq.2)}$$

The seismic dataset obtained after a seismic survey and its fundamental properties, such as the seismic resolution, are principally determined by the acquisition parameters and by the system characteristics (in particular its frequency spectrum). After acquisition, the next step is data processing, and this step can significantly improve the image resolution and attenuate unwanted noise within some limits. The resolution, in a general way, can be defined as the ability to distinguish two very closely distinct objects. The seismic resolution is directly related to the

frequency and duration of the pulse. Power sources that emit high-frequency pulses have higher resolution and therefore a greater ability to detect thin layers.

Thus, seismic resolution is a matter of major importance in seismic data acquisition (Yilmaz, 2001). UHRS (Ultra High Resolution Seismic) data was used in this work, and normally has a denser data acquired and contains a range of frequencies above 500 Hz to 5kHz.

Vertical resolution

The vertical resolution of the seismic wave is defined as the minimum thickness of a layer required to distinguish a reflection from its top to the base, i.e. the ability to recognize individual, closely-spaced distinct reflectors. The vertical resolution is determined by the pulse length (or frequency) of the seismic system. The seismic frequency is directly related to the vertical resolution: higher frequency provides higher resolution. The frequency is expressed as number of cycles per second (1cycle/s = 1Hertz) and higher frequencies mean shorter pulses and consequently better vertical resolution (Sheriff and Geldart, 1995; Kearey et al. , 2002).

The top and the base of a stratigraphic unit (two distinguish reflectors), can be recognized as separated seismic events only if the distance between them is at least ¼ of wavelength (λ) of the seismic wavelet (Equation 3; McQuillin et al., 1984).

$$\lambda = \frac{V}{f} \qquad \text{(Eq.3)}$$

Where *V* is the seismic wave velocity in the layer and *f* is frequency.

As the waves travel in the subsurface, the seismic wave will lose the highest frequencies in depth, because they are more rapidly absorbed. Thus, high-frequencies waves are attenuated much faster than low-frequencies. The higher frequency, the lower will therefore be the depth penetration, but the higher will be the vertical resolution.

Horizontal resolution

The horizontal resolution of a seismic wave is principally controlled by the “1st Fresnel Zone” that consists of the area of the sub-surface that contributes to the reflection. A reflection that is coming back to the surface is being reflected not from a reflecting point, but from an area with the dimension of the “First Fresnel Zone”.

The “First Fresnel Zone” according to the Huygens’s principle is an area where the waves interfere with each other constructively. This principle also states that each part of a wave front acts as a source of a new wave (Sheriff and Geldart, 1995).

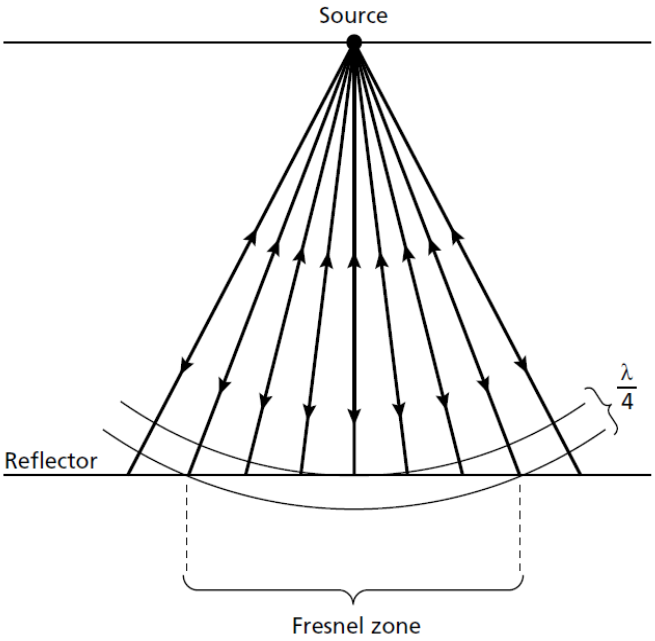

Figure 3. Schematic representation of the First Fresnel Zone (Kearey et al., 1991).

As shown in Equation 4, the radius of the 1st Fresnel Zone (FR) depends on the average seismic velocity on the layer (V), the depth of the target (*t*, in TWT) and the frequency of the seismic signal (f) (Sheriff and Geldart, 199). The Fresnel zone increases, and consequently horizontal resolution decreases, with increasing velocity of the propagating medium and travel-time (depth), and also with lower signal frequency.

$$FR = \frac{V}{2} * \sqrt{\frac{t}{f}} \qquad \text{(Eq.4)}$$

Diffractions

The presence of discontinuities at the interfaces between the various layers, for example due to the presence of faults (Figure 4) or a very irregular topography of the reflecting interface, generates diffractions, which appear in the seismic sections as hyperbolae. These diffractions appear because the interface between the formations truncates abruptly, then secondary waves do not cancel at the edge, and diffraction is observed (Huygens’s principle). In data processing with migration, it is possible to collapse the hyperbolae.

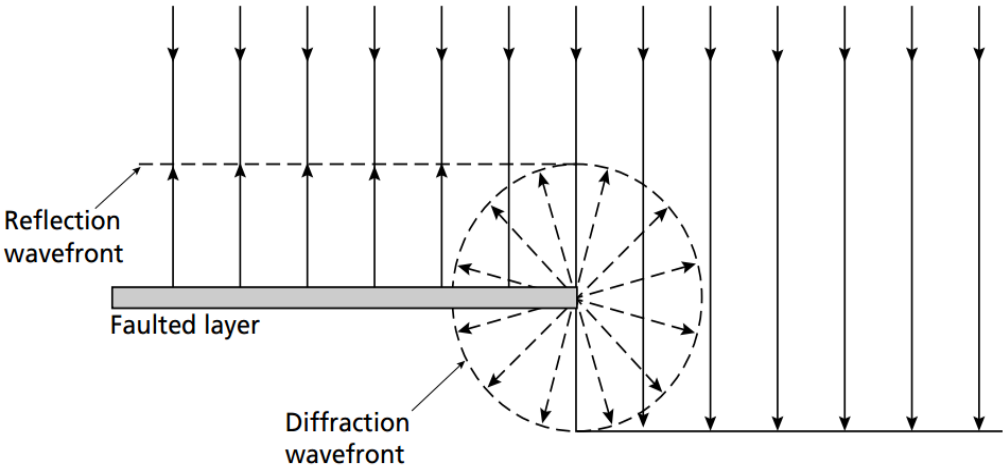

Figure 4. Schematic image of the diffraction caused by the truncated end of a faulted layer (Kearey et al., 2002).

Multiples

The presence of multiple reflections in the seismic sections due to reflections, for example at the water / air interface in a marine environment or multiple internal reflections in the various layers in the presence of strong acoustic impedance contrasts, makes interpretation very difficult. They can be attenuated with special processing techniques (i.e. during the stack), but their total removal is a virtually impossible task – significant advances in processing have however been achieved in recent years. There are diverse types of multiple reflections as can be seen in Figure 5.

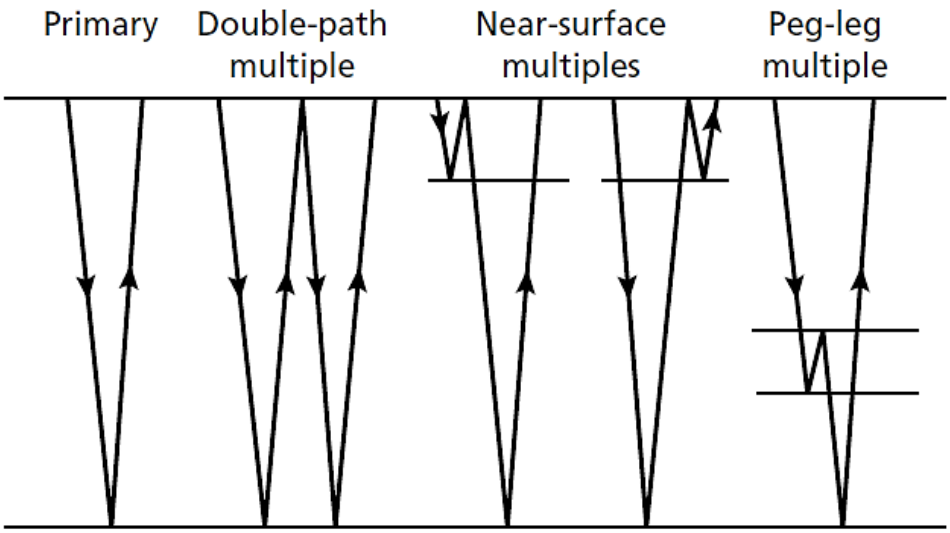

Figure 5. Distinct types of multiple reflection in a layer (Kearey et al., 2002).

2.2 Seismic Data Acquisition

In the acquisition of multi-channel seismic reflection data in marine environment, a streamer of hydrophones and a seismic source are towed behind a ship. The streamer will be receiving the reflected waves from the subsurface and convert them into electrical signals.

In the 2D seismic marine acquisition, a single streamer is used (Figure 6 A); in 3D seismic marine acquisition several streamers are towed behind the vessel (Figure 6 B), and the shooting direction (boat track) is called the inline direction (Yilmaz, 2001). The three-dimensional (3D) seismic acquisition method appeared only in 1972, when the American G.G. Walton presented it for the first time to the scientific community.

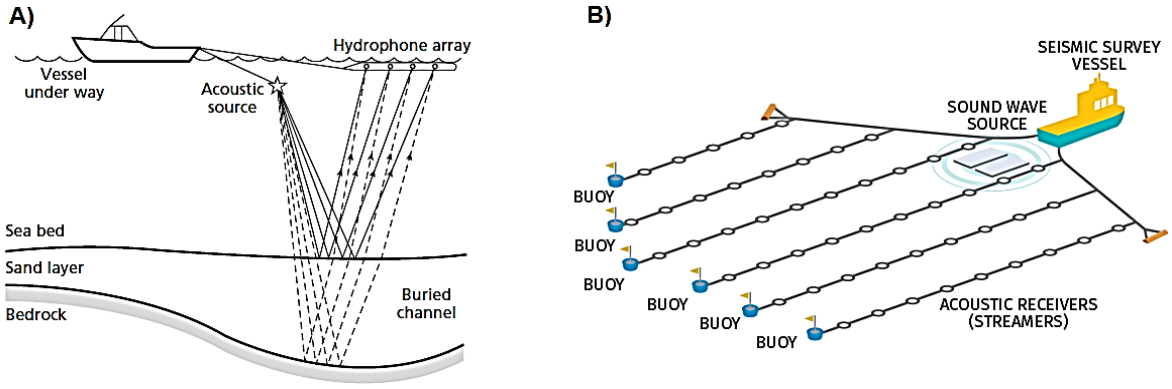

Figure 6. Schematic images the two types of seismic acquisition on sea. A) 2D seismic acquisition (Kearey et al., 2002). B) 3D seismic acquisition (http://wikigrewal.com/offshore-marine-seismic-surveying/).

The 3D seismic marine acquisition has several advantages over the two-dimensional seismic acquisition: it resolves the structural and stratigraphic details of the subsurface that were missing or were simply not visible in 2D seismic, and therefore it is possible to visualize the potential reservoirs (oil and gas) in three dimensions, allowing the interpreter to obtain detailed information on faults and fractures, stratification planes, presence of pores and fluids, complex structural geology and detailed stratigraphy. It also allows correct positioning of the reflectors in 3D.

Although the 3D seismic marine acquisition has several advantages, it is more expensive, and requires more sophisticated and more expensive equipment, and therefore it takes more time to check if all the equipment, including the multiple streamers, is working and ready for acquisition. The 3D seismic marine acquisition is a complex method and therefore the acquisition geometry is also complex if good azimuth illumination coverage is intended.

The traditional geometry used in 3D data acquisition uses lines previously delineated over the area of interest. After completing each navigation route, the vessel goes to the next acquisition line, (transit time), in the opposite direction, parallel to the previous one (Figure 7 A). During the change of direction/acquisition line there will be a change in the position of the sources and receivers resulting in non-productive time.

For the optimization of non-productive time, new acquisition geometries were developed. As an example, we have Wide-Azimuth (Buia et al., 2008) and Coil Shooting (Buia et al., 2008).

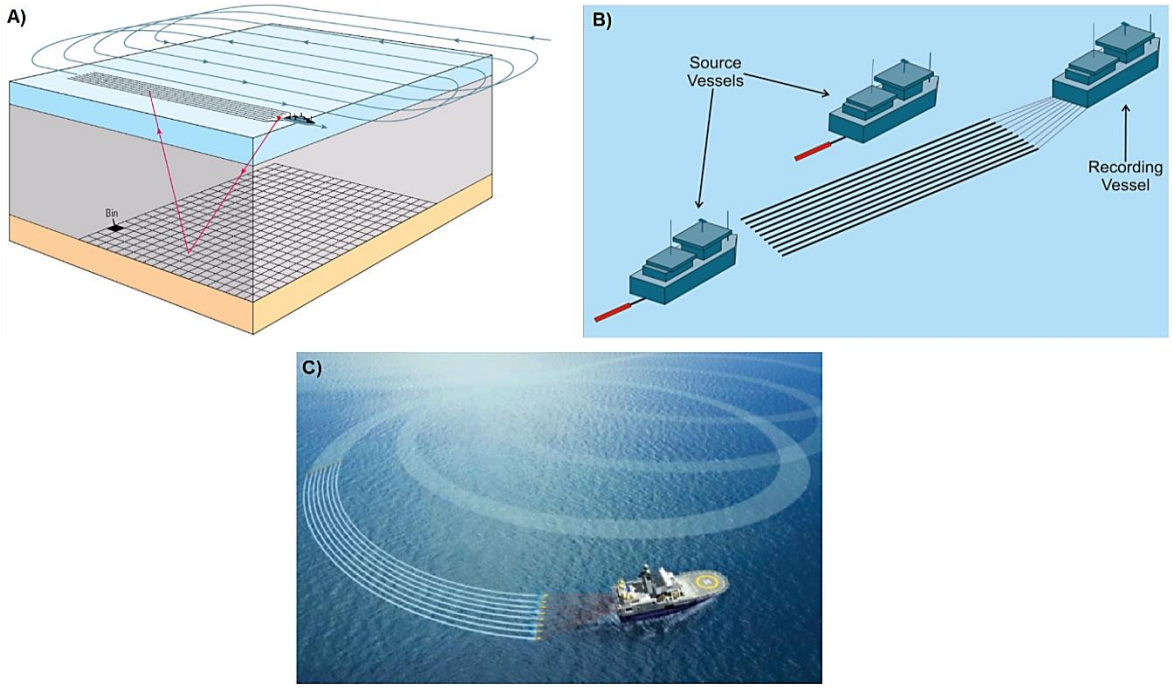

Figure 7. Schematic images of the three type's ways to make a 3D seismic acquisition on sea. A) The basic 3-D Acquisition, this is the most traditional way (Buia et al., 2008). B) The Wide-azimuth survey (Buia et al., 2008) C) The Coil shooting acquisition technique (Buia et al., 2008).

In Wide-Azimuth (Figure 7 B) the same acquisition pattern is used as in the traditional acquisition, but with several vessels that shoot sequentially in different directions for the same streamers, which allows better azimuthal coverage of the study area. This method proved to obtain better data namely, less noise, better resolution, improvements in the attenuation of multiples and the quality of the reflectors, simplifying the seismic interpretation (Buia et al., 2008).

The Coil Shooting (Figure 7 C) is a technique, proposed by the company Schlumberger, for seismic acquisition that uses a circular pattern for data collection, with little or no unproductive time. It allows getting data of short offsets, something not possible by the traditional geometry and involves only a single ship equipped with several seismic sources and streamers, and that runs a

continuous circular trajectory on the study area (Buia et al., 2008). In circular geometries, we obtain azimuth coverage values in the order of 90% while in parallel line geometries the acquisition productivity drops to approximately 45%. From the economic point of view, it is more lucrative to use the WAZ method in large areas of exploration and Coil Shooting in small/medium areas (Buia et al., 2008).

2.2.1 Marine Seismic Sources

There is a wide variety of seismic sources characterized by diverse levels of energy, typical frequencies and method of operation. Frequencies of the seismic sources can range from 1Hz to several hundred or even thousands of hertz (Figure 8).

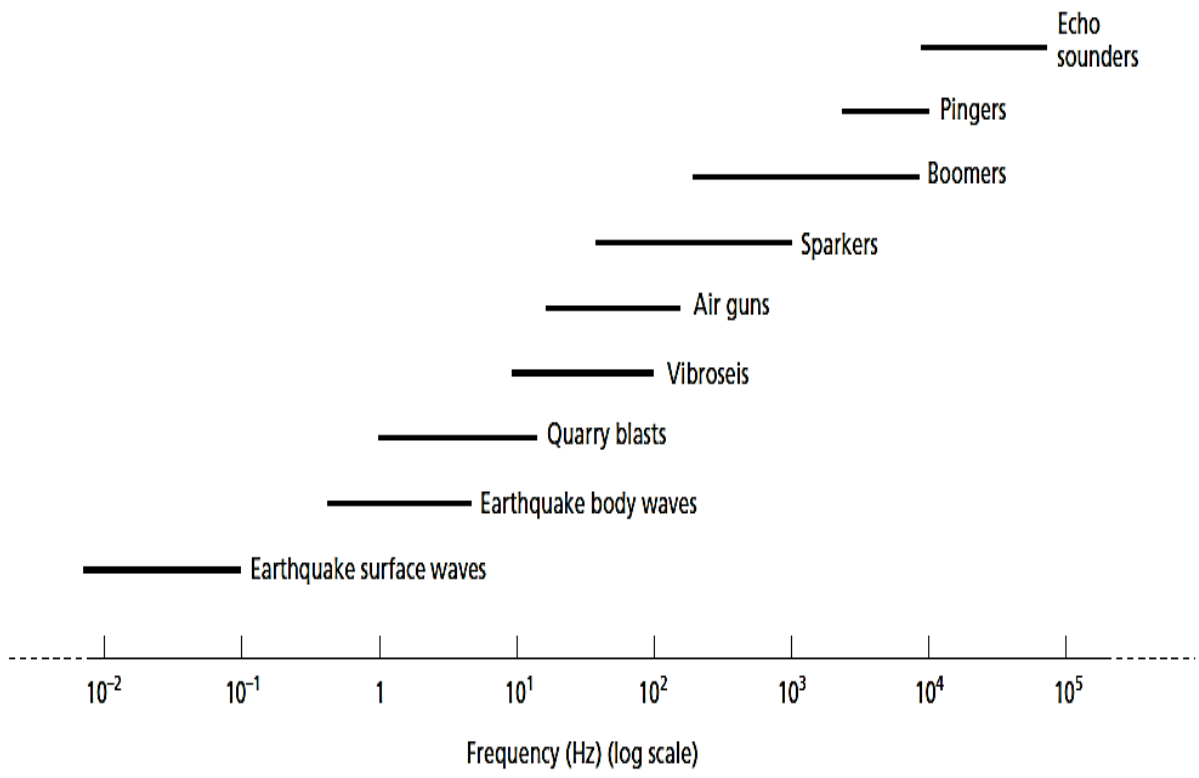

Figure 8. Acoustic spectrum of different seismic sources (Kearey et al., 2002).

The data used in this master thesis came from a high frequency seismic source, in this case, a Sparker. The sparkers are equipment's that convert electrical energy into acoustic energy, through a pulse that is generated by the discharge of a large capacitors to create a spark between two electrodes inside conducting water.

The operating voltages are characteristically 3.5–4.0 kV and peak currents may exceed 200 A. This electrical discharge leads to the formation and rapid growth of a plasma bubble and the consequent generation of an acoustic pulse (Kearey et al., 2002).

2.2.2 Marine Seismic Receivers

In order to receive and record the reflected seismic waves when the acquisition campaigns are made at sea, streamers are used, which are arrays of hydrophones, distributed over several channels along an extensive plastic tube filled with a liquid that allows the streamer keep to the surface.

The hydrophones are composed of ceramic piezoelectric elements (Figure 9) which produce an output electrical signal (voltage) proportional to the pressure variations associated with the passage of a compressional seismic wave through water.

The sensitivity of this equipment is typically 0.1mVPa^{-1} (Kearey et al., 2002). Each crystal element consists of an annular piezoelectric ring, metallic-coated on both surfaces, bonded at the open ends by thin convex metallic diaphragms.

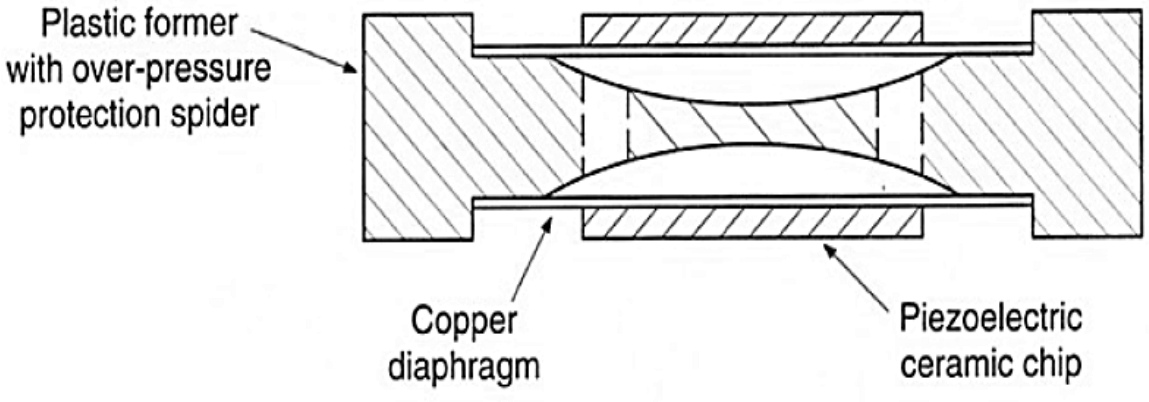

Figure 9. Schematic image of hydrophone (adapted from Reynolds, 1997).

2.3 Basic Seismic Data Processing

The typical seismic processing flows are implemented to increase the seismic vertical resolution, improve the signal-to-noise ratio of the data and to display the seismic events in their correct spatial position (Yilmaz, 2001; McQuillin et al., 1984; Kearey et al., 1991).

A typical processing flow for a 2D survey is composed by a first part known as the pre-processing stage, and a second part which constitutes the specific processing flow. The pre-processing includes: demultiplexing, quality control, trace editing, filtering, spherical divergence and gain corrections, and geometry and static corrections; the second part normally includes: deconvolution, filtering, CMP sorting, velocity analysis, normal moveout (NMO) correction, CMP stack and migration (Yilmaz, 2001). The first step in pre-processing is to perform the demultiplexing, an operation that consists of reorganizing the data to a format appropriate for processing as shot gathers. Conventionally, in the oil industry the SEG-Y format is used to store and share seismic data (Yilmaz, 2001).

In the quality control phase, the traces that are recognized by the operator as anomalous (noisy or inverted polarity) are eliminated so as not to compromise the remaining data. A basic filter is also applied to eliminate the noise characteristic of low frequencies caused by bad atmospheric conditions or undesired streamer movements, for example, cable feathering (Yilmaz, 2001).

The correction of spherical divergence is a function that applies some gain to compensate for the loss of amplitude of the seismic energy as it moves away from the source inside the Earth, by increasing the gain of the signal with increasing distance. This correction must be used when considering large distances, for small distances requires some care in their use as it can greatly increase noise instead of improving data.

After the data is corrected, it is ready for the definition of the acquisition geometry in the field, positioning the sources and receivers in the trace headers. This step is the one of the most important phases of the processing, and may lead to many problems if a wrong definition of parameters is used.

The recorded seismic trace is a convolution of the seismic wavelet with the reflection coefficient series which result from the contrasting properties (density and seismic velocity) of the different rock layers, where the seismic rays pass through.

The deconvolution it is an inverse filtering technique used to compress an oscillatory (long) source waveform, often seen on marine data, into a spike (unit-impulse function), as close as possible. This technique allows eliminating some noise that was convolved during the acquisition, for instance, the source signature and derived multiples, obtaining the reflection coefficient series of the geological formations, once the shape of the wavelet is made closer to a peak of energy. The great advantage of deconvolution is to increase the vertical resolution by compressing the wavelet without compromising the frequency content. This procedure leads to a significant improvement of the seismic profile but can also increase high frequency noise and may require subsequent filtering (Yilmaz, 2001).

The velocity analysis is performed on selected CMP gathers (Figure 10) or group of gathers (Super Gathers). The velocity model is then used to correct the NMO of the CMP gathers and afterwards in migration.

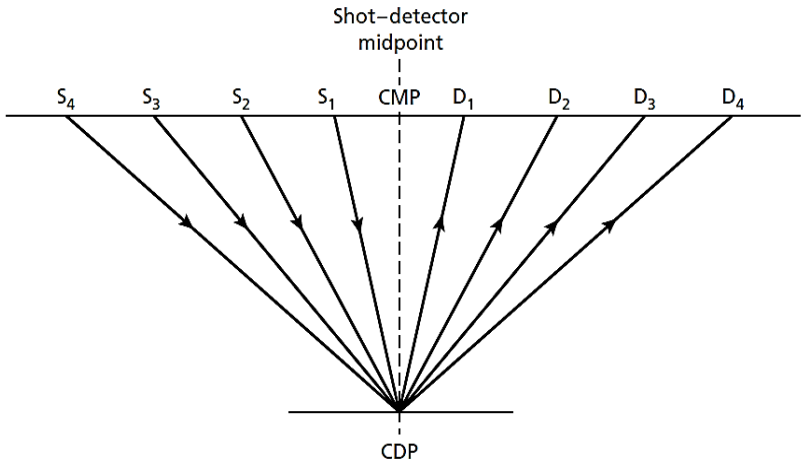

Figure 10. Common mid-point (CMP) reflection profiling. A set of rays from different shots (Si) to detectors (Di) reflected off a common depth point (CDP) on a horizontal reflector (Kearey et al.,2002).

The NMO correction is applied to correct differences in distance between the source and the receiver inside the same CMP's family (Figure 11 A), in a non-dipping reflector, assuming that the propagation distance as a function of time describes a hyperbolic trajectory; the goal of NMO correction is to remove the curvature of this reflection hyperbola (Yilmaz, 2001).

After the NMO correction (Figure 11 B) of the CMP gather, the next step of the typical processing flow is the CMP Stacking (this is possible because, the data came from multi-channel seismic acquisition with multiple CMP coverage). The Stack (Figure 11 C) consists of summing the traces which belong to the same CMP location into just one trace at normal incidence, after NMO

correction. This process will increase the signal-to-noise ratio and attenuate noise such as multiples and ground roll, because the reflected signal and coherent noise usually have different stacking velocities (Yilmaz, 2001).

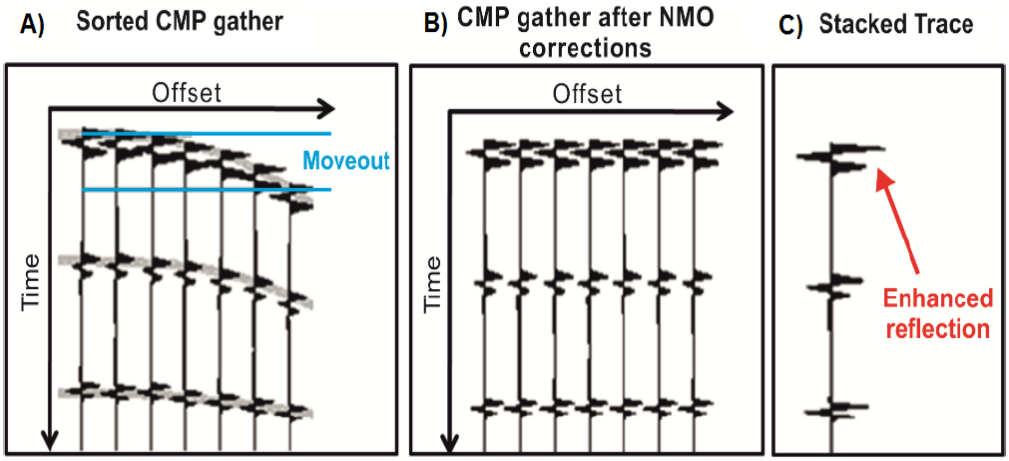

Figure 11 . A) Sorted CMP gathers; every Si-Ri that corresponds to the same reflection point; B) CMP gather after executing the NMO corrections; C) Stacked trace with a better signal (from http://www.gsj.go.jp, modified by Ribeiro, 2011).

The standard processing flow usually finishes with a migration. This process moves the seismic reflectors to their correct position in space, if the realistic velocity model is calculated. The migration process will move the dipping events into their supposedly true subsurface positions, collapse the diffractions, increase the spatial resolution and correct amplitudes for geometric focusing effects (Yilmaz, 2001). This process can be applied after (post-stack migration) or before the stack (pre-stack migration).

The pre-stack migration it is a heavy computational process and takes a long time to complete. The algorithm is applied trace to trace at each CMP location, instead of being applied to the stacked data (Yilmaz, 2001). The pre-stack migration produces an image of the subsurface with superior quality, allowing the user a better interpretation of the area under study.

The main differences between the 2D seismic data processing and 3D seismic data processing are: quality control, statics correction, velocity analysis, migration and the way in which reflective points are considered for seismic processing purposes. All the processing steps (either in 2D seismic data processing or 3D seismic data processing) should be quality controlled through the seismic processing job to ensure that the quality of the data is not diminishing during the seismic data processing. Cable feathering is caused by cross currents, and in marine 3-D surveys can result

in travel time deviations from a single hyperbolic moveout within a common-cell gather (Yilmaz, 2001).

As described previously, the 2D seismic processing, requires first sorting the recorded data into common midpoint gathers, and in a similar form, the processing of 3D seismic data requires *Binning* the recorded the traces into common cell gathers (*bins*) to create common-cell stacks. A common-cell gather coincides with a CMP gather for swath shooting. For marine surveys, the typical cell sizes are 12.5 × 25 m (Yilmaz, 2001).

For a surface subdivided by a grid of lines, the area between adjacent lines is called a *Bin*. The traces which fall within a *bin* are assumed to lie at the *bin* centre, which is also called a node or grid cell. The *Binning* is sorting traces into the appropriate *bin* (Sheriff, 2002).

The traces are assigned to specific *bins* according to the midpoint (Middle Point) between the source and the receiver (Figure 12). *Bins* are commonly assigned according to common midpoint (CMP), but more sophisticated seismic processing allows for other types of *Binning*. Traces within a *bin* are stacked to generate the output trace for that *bin*. Data quality depends in part on the number of traces per *bin*, or the fold.

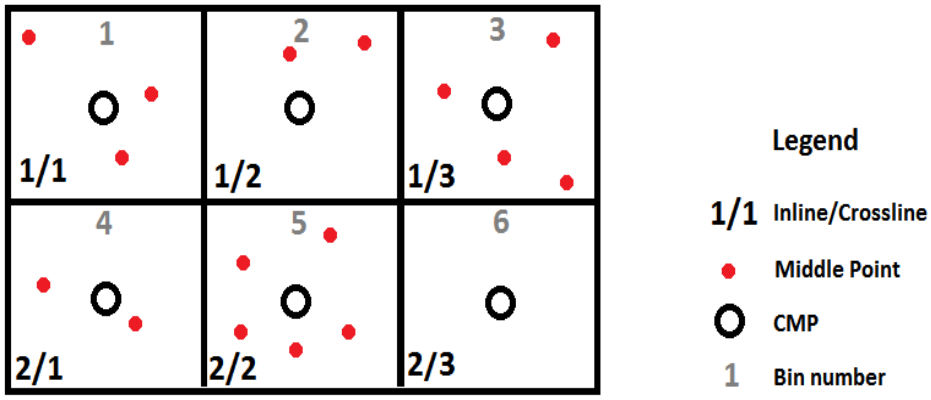

Figure 12. Schematic image about what contains a *bin*.

Conventional 3-D recording geometries often complicate the process of stacking the data in a common-cell gather. After stacking, the 3-D data volume is migrated. Before migration, the data sometimes needs to be trace-interpolated along the crossline direction to avoid spatial aliasing (Yilmaz, 2001). The migrated 3-D data volume then is available to the interpreter as vertical sections in both the inline and crossline directions and as horizontal sections.

3.The Hornsea Offshore Windfarm Project One - 3D UHRS Survey – Case Study

As referred to in Chapter 1, the study area is located in the southern North Sea. In order to make the reader first acquainted with the geological setting of the seismic survey, this Chapter starts with a brief summary of the geological setting of the study area and its geological evolution. This is followed by a description of the seismic survey details and the presentation of some images of the resulting seismic block, in which the main seismic horizons are interpreted.

3.1 Geological Framework of the Southern North Sea

Hans Stille, in 1924, divided the European continent into four major domains according to the time of the orogenic stabilization, based on the last orogeny that affected them: the Eo-Europe (Precambrian Europe), the Paleo-Europe (Caledonian Europe), the Meso-Europe (Variscan Europe) and the Neo-Europe (Alpine Europe). The Southern North Sea is inserted on Paleo-Europe, without significant deformation since the end of the lower Paleozoic (Figure 13).

The Southern North Sea Basin has a complicated and vast history of geological events, namely basinal subsidence. The basinal subsidence has been interrupted by distinct episodes of uplift and widespread erosion.

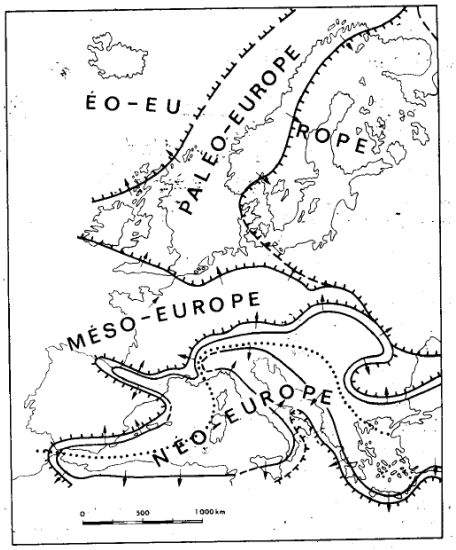

Figure 13. Main tectonic units of Europe, based on Stille (1924) and modified by Ribeiro et al., 1979.

3.1.1 Paleozoic (541-252.1 Million years ago)

Throughout most of the southern North Sea the lower Paleozoic sediments intruded by granite plutons and mildly deformed during the Caledonian Orogeny of Late Silurian to Early Devonian approximately 420 - 390 million years ago (Balson et al., 2001; Cameron et al., 1992).

The predominantly WNW and NW trends of the faults within the Late Paleozoic, Mesozoic and Cenozoic sequences may be hereditary from the structure of the fundamental Lower Paleozoic basement (Balson et al.., 2001).

Following the Caledonian uplift, most of the Southern North Sea remained an area of erosion under the sea about 410-360 million years (Devonian). Crustal extension started early in the Carboniferous approximately 360 million years ago, which allowed the deposition of deltaic sediments within the graben areas (Cameron et al., 1992).

Some of the granite batholiths inferred from their geophysical signatures may lie beneath early Carboniferous horsts (Cameron et al., 1992), though expressively different interpretations exist for the locations of the syn-rift blocks and basins (Collinson et al., 1993; Besley, 1998). The rifting had effectively ceased and a phase of thermal subsidence had commenced, around 325 million years ago (Balson et al., 2001).

During the Variscan Orogeny about 300-290 million years ago, the Carboniferous rocks were moderately folded and faulted. About 310 - 270 million years ago, a differential Late Carboniferous to Early Permian regional uplift led to the erosion of more than 1500 m of Carboniferous strata from parts of the Southern North Sea Basin (Balson et al., 2001).

The southern North Sea Basin, after the Variscan Orogeny, began to subside again in the Permian times, and more than 2700 m of Permo-Triassic levels, covering an age range of around 290-210 million years were deposited, including red beds and a thick, cyclical, evaporite succession (Ziegler, 1975; Balson et al., 2001).

3.1.2 Mesozoic (252.1-66.0 Million years ago)

The Late Triassic and Early Jurassic subsidence in the Sole Pit Basin was related to the reactivation of its Variscan basement faults (Glennie and Boegner, 1981). These tectonic movements generated the earliest mid-Triassic halokinesis of the Upper Permian salts (Balson et al., 2001).

The marine conditions were then re-established in the southern North Sea at the end of the Triassic. Then, during early–mid Jurassic times, differential subsidence of the Sole Pit Basin was accentuated by the extensional faults along the western margin. It is these faults that account for the major thickness of the Lower and Middle Jurassic sediments between the East Midlands Shelf and the Sole Pit Basin (Balson et al., 2001).

In the Middle Jurassic, widespread domal uplift centreed in the central North Sea and resulted in an erosional unconformity. More than 1000 m of Jurassic and Triassic strata were eroded from the Cleaver Bank High at this time (Glennie, 1986). During the Late Jurassic, there was a widespread pulse of diapirism (Glennie and Underhill, 1998; Balson et al., 2001).

Lower Cretaceous sediments are typically less than 200 m thick, but reach up to 1000 m in local zones of growth faulting, associated with sinistral fault movement (Kirby and Swallow, 1987). During the Late Cretaceous, the Cleaver Bank High became established as the main depo*centre* and accumulated more than 1000 m of Upper Cretaceous chalk (Balson et al., 2001).

The Upper Cretaceous chalk formations include cemented carbonate platforms of chalk crop at seabed. Chalk is an important aquifer in the onshore and offshore margins of the southern North Sea where it covers large areas (Balson et al., 2001).

3.1.3 Cenozoic (66.0-0.0 Million years ago)

The Sole Pit Basin and the Cleveland Basin are two examples of basins from NW Europe that have been affected by basin inversion during, or at the end of, the Late Cretaceous. This basin has been attributed to strike-slip reactivations of basement faults (Glennie and Boegner, 1981; Balson et al., 2001).

Cenozoic subsidence in the North Sea has been controlled by broad synclinal down warping towards a depositional axis that extends from the Viking Graben, through the Central Graben in the direction of the Netherlands (Balson et al., 2001).During the Cenozoic, the basin was lightly deformed by tectonic inversion and basin-margin uplift driven by intraplate compression, resulting from the interplay between the opening of the NE Atlantic Ocean and the Alpine orogeny (Caston, 1977; Graham et al., 2011).

During Oligocene to Miocene times, many of the basement faults in the Southern North Sea were reactivated by dextral strike-slip (Glennie and Boegner, 1981), which triggered further major

halokinesis. Most of the salt pillows north of 54^{o} north were initiated in mid-Cenozoic times, and Glennie (1986) connected contemporaneous inversion of the Sole Pit Basin to Alpine movements. There are very few Miocene sediments and Pliocene deposits too (Balson et al., 2001). Since the Mid-Cenozoic, up to 3000 m of Oligocene to Holocene sediment has accumulated in the central graben region, including, locally, more than 800 m of Quaternary sediment (Caston, 1977; Graham et al., 2011).

Rapid subsidence became more widespread early in the Quaternary resulting in the preservation of more than 600 m of Pleistocene progradational delta deposits and glaciogenic deposits (Balson et al., 2001).

The Quaternary climatic change was a major event in the recent history and is preserved in the sedimentary record of the southern North Sea; during the colder periods it exhibited mean annual air temperatures well below zero degrees Celsius (Plant et al., 2003). The major effects of this event are erosion and deposition of material over large parts of the continents and surrounding seas, modification of the river systems, creation of multiple small bodies of water, major changes in sea level and isostatic adjustment of the crust (Long et al., 1988). This has affected the type of deposits available to be preserved on the geological record and their properties.

Unfortunately, most terrestrial evidence for most of some 25 such glacial cycles, recognized in marine sediments, has been destroyed by subsequent events. The surviving geomorphological and stratigraphically record is usually restricted to deposits of the main *glacial* events, which are the Elsterian, the Saalian and the Weichselian glaciations (Figure 14; Long et al., 1988).

The Quaternary of the British sector of the North Sea has been divided into several groups, as described below.

Crag Group

The base of quaternary in British sector of the North Sea is now taken at the top of the Red Crag Formation, an Upper Pliocene formation consisting of shell-bearing glauconitic sediment, which occurs at or near bed off the coast of East Anglia (Long et al., 1988; Stoker et al., 2011). The Red Crag Formation is the only offshore formation of the Crag Group. This formation is a high-energy shallow-marine glauconitic deposit, and therefore lithologically like to the onshore formation with the same geological time.

The Red Crag Formation might range in age from Late Pliocene to Early Pleistocene, around to 3.2–2.4 Ma, based on the presence of the planktonic foraminiferid (Funnell, 1988). It is rests with marked unconformity on Palaeogene or Neogene formations and is unconformably overlain by deposits of the Southern North Sea Deltaic Group (Cameron et al., 1992; Stoker et al., 2011).

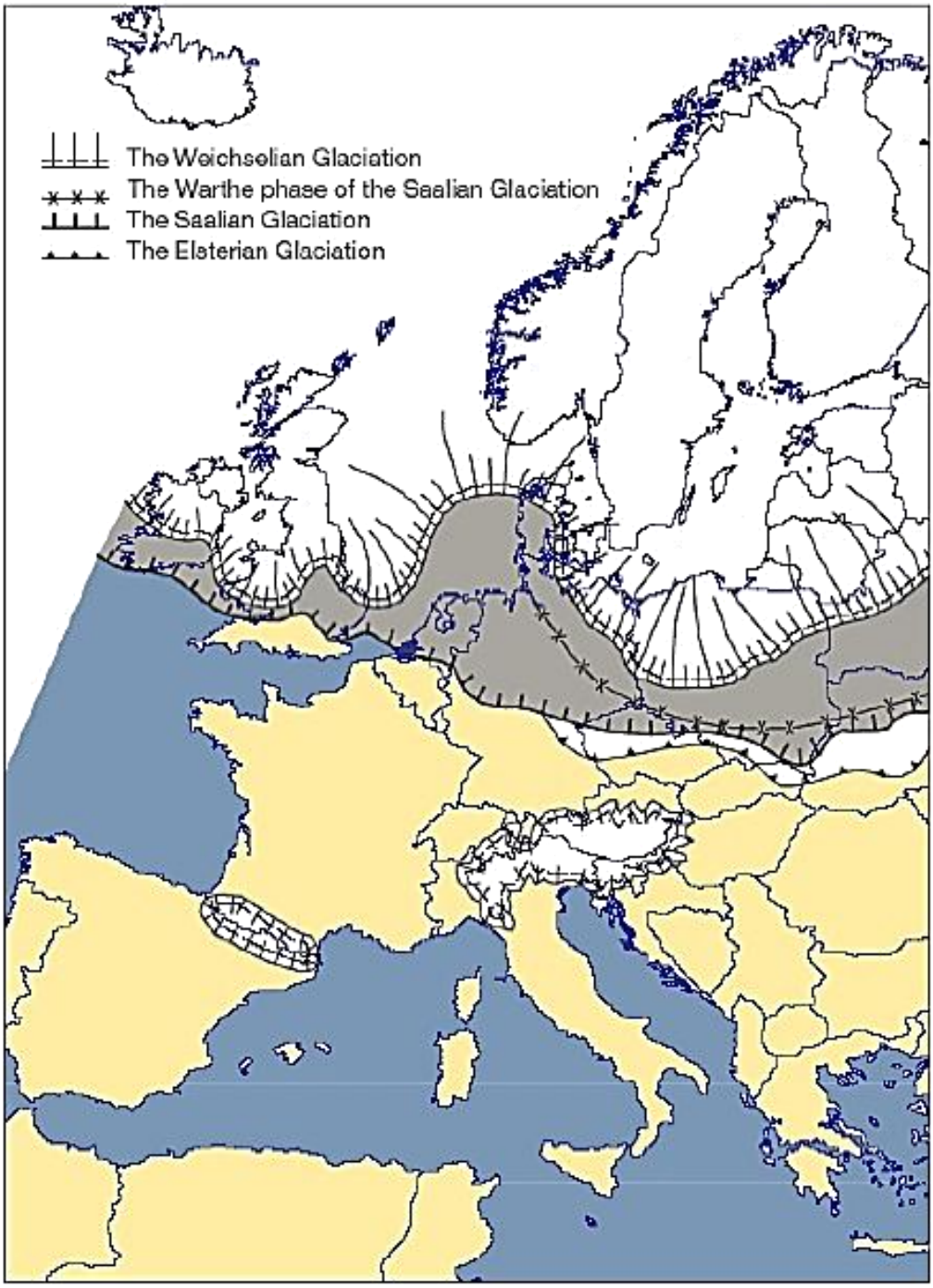

Figure 14. Map of the North Europe, showing the maximum extension of the European ice sheets: the Elsterian, the Saalian and the Weichselian glaciations (from Anderson and Borns, 1997).

Southern North Sea Deltaic Group

In the British sector (Figure 16), the Lower to early middle Pleistocene succession displays seismic facies that can relate to a specific environment, a delta complex (Long et al., 1988). The Southern North Sea Deltaic Group is defined essentially nine constituent formations: the Westkapelle Ground, Crane, Smith's Knoll, Ijmuiden Ground, Winterton Shoal, Markham's Hole, Outer Silver Pit, Aurora and Batavier formations. These formations succeed each other northwards as the delta prograde into the basin. The base of the Southern North Sea Deltaic Group is around Early Pleistocene, and mostly overlies the Red Crag Formation, though the latter may be partly correlated with the Westkapelle Ground Formation (Stoker et al., 2011).

The term Southern North Sea Deltaic Group is proposed for a thick succession of marine deltaic formations, including delta front and prodelta deposits (apart from the Crane Formation), formed by sediments derived from south eastern England and the Netherlands that are preserved in the Southern North Sea (Stoker et al., 2011).

The deltaic and pro-deltaic sediments from this group are associated with the development of the southern North Sea delta, which has been compared in size to the largest modern delta complexes in the world (Ekman and Scourse, 1993), and was accountable for the majority of non-glacial deposition during the Early to Mid-Pleistocene in the southern and central North Sea (Cameron et al., 1992; Graham et al., 2011; Stoker et al., 2011).

The union of the two delta fronts occurred in earliest Beestonian (Eburonian) times, when the direction of advance swung northwards (Cameron et al., 1992; Stoker et al., 2011; Long et al., 2011). The top deltaic group is diachronous with the Yarmouth Roads Formation, which is here assigned to the Dunwich Group (Cameron et al., 1992; Stoker et al., 2011; Long et al., 2011).

Dunwich Group

The Yarmouth Roads Formation is the only offshore formation to be assigned to the Dunwich Group, which has been correlated in part with the Sudbury Formation of the Kesgrave Catchment Subgroup in East Anglia (onshore). The base is highly diachronous being oldest (Beestonian/Waalian) in the south, and becoming less easily definable towards the centre of the basin, where it is locally coeval with the fully marine formations of the Southern North Sea Deltaic Group. The formation was deposited prior to the Anglian (MIS 12) and is unconformably overlain by the California Glacigenic Group **(**Cameron and Holmes, 1999; Stoker et al., 2011).

California Glacigenic Group

Generally, glacier related deposits are preserved in the sedimentary record of the southern North Sea by moraine, glaciofluvial and glaciolacustrine deposits from the Elsterian, Saalian and Weichselian glacial periods (Figure 14). At these times, the British and Fennoscandian ice sheets covered certain amounts of the area, contributing to the erosion, supply of sediments and infill of this basin (Stoker et al., 2011; Long et al., 2011).

The California Glacigenic Group consists essentially in 16 formations. The base of this group is marked by the Swarte Bank Formation. The Swarte Bank Formation is located in the base of buried valleys in the southern North Sea Basin, south of 55°N (Davies et al., 2011). During the Elsterian glacial period (MIS 12), full glacial conditions led to the erosion and infilling of a major system of tunnel valleys, up to 12 km wide and 400 m deep, in the southern North Sea Basin (Cameron et al., 1987).

The infilling of the valleys commenced with stiff glacial and glaciofluvial sand, overlain by glaciolacustrine muds and culminating with marine interglacial sediments of the Sand Hole and Egmond Ground formations. The age of the infilling deposits therefore is from late Anglian to earliest Hoxnian (Stoker et al., 2011).

The Cleaver Bank and Tea Kettle Hole formations happen near to the centre of the southern North Sea, they are both of Wolstonian age (Figure 15). The Cleaver Bank Formation is a partly marine proglacial diamicton with clasts derived from the east (Cameron et al., 1992), but also includes glaciolacustrine and glaciofluvial facies. The Tea Kettle Hole Formation is broadly contemporaneous with the Cleaver Bank Formation, and consists of discontinuous deposits of periglacial aeolian sands. These units are overlain by the interglacial Eem Formation (Stoker et al., 2011).

The earliest set of glacigenic units consists of seven formations: the Well Ground, Bolders Bank, Dogger Bank, Botney Cut, Twente, Sunderland Ground and Hirundo formations, which are all Devensian. Periglacial, fluvial deposits comprise the Well Ground Formation.

Climatic deterioration towards fully glacial conditions caused regional sea level in the North Sea to fall to at least 110 m below present by late Weicheselian glacial period. A blanket deposit of Weichselian is the Boulders Bank Formation. This formation is a widespread deposit of diamicton believed to have been deposited by a lobe of ice which moved down the east coast of England (Cameron et al., 1987).

The Bolders Bank Formation (Figure 16) interfingers with proglacial sediments of the Dogger Bank Formation. Previous micromorphological investigation of the Bolders Bank Formation indicated genesis as a subglacial till (Carr et al., 2000), reflecting an ice sheet extending across the southern North Sea (Davies et al., 2011). Subglacial valleys were incised into older Pleistocene sediments and have partially been infilled by the diamictons of the Botney Cut Formation (Stoker et al., 2011).

The Twente Formation represents periglacial wind-blown sands deposited near the ice margin. Late-stage infilling of troughs as the ice retreated westwards occurred with the glaciolacustrine to glaciomarine sediments of the Sunderland Ground and Hirundo formations (Stoker et al., 2011). As already mentioned, there are a few formations that corresponds some marine interglacial units. These units are represented by six constituent formations, namely, the Sand Hole and Egmond Ground formations are Hoxnian (Holsteinian interglacial period); the Eem and Brown Bank formations are Ipswichian to Early Devensian; and the Elbow and Southern Bight formations are Holocene (Stoker et al., 2011).

The Sand Hole Formation is confined to an area around the modern Inner Silver Pit. In contrast, the Egmond Ground Formation occurs widely and may infill the uppermost portions of Anglian subglacial valleys overlying the Swarte Bank or earlier deltaic formations such as those of the Dunwich Group. A stratigraphical break due to the fall in sea level during Wolstonian times separates these formations from those of the next marine incursion during Ipswichian times (Stoker et al., 2011).

The marine sediments of the Eem Formation (Eemian interglacial period) have been identified at several sites and are made of intertidal and shallow marine sands and clays. This formation rests unconformably on the Egmond Ground Formation and is overlain by a marginal marine deposit, the Brown Bank Formation, which may have been deposited as sea levels fell during Early Devensian times equivalent to MIS 4 (Cameron and Holmes, 1999). A further stratigraphical break separates these formations from the deposits of the postglacial return of marine conditions into the southern North Sea (Stoker et al., 2011).

Finally, the earliest Holocene brackish-marine incursion into the southern North Sea may have occurred as early as 10 ka BP (Eisma et al., 1981). The earliest Holocene is characterized by the Elbow Formation; this formation was deposited in shallow water intertidal or coastal environments.

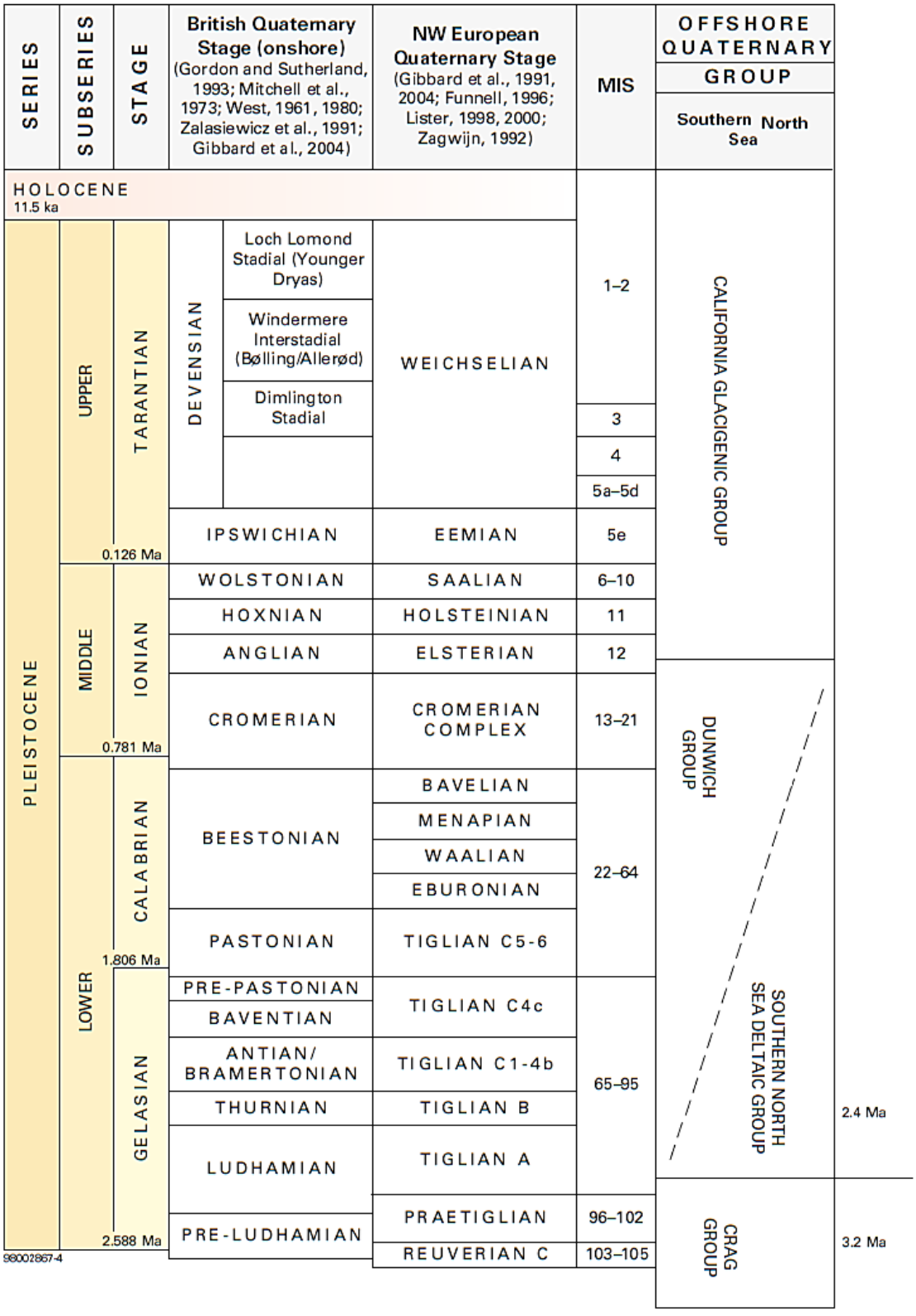

Figure 15. Summary of the Quaternary lithostratigraphical framework for the UKCS with relationships of groups to Quaternary stages, suggested correlation with Marine Isotope Stages (MIS), and correlation with onshore framework (modified by Stoker et al., 2011).

As fully open marine conditions became established the Elbow Formation was overlain unconformably by the deposits of the Southern Bight Formation, which contains a number of diachronous members. These members include transgressive deposits that formed around 8000 BP (Eisma et al., 1981; Long et al., 1988) and the modern mobile marine sediments, such as those found within sandwaves or sandbanks in the southern North Sea (Stoker et al., 2011).

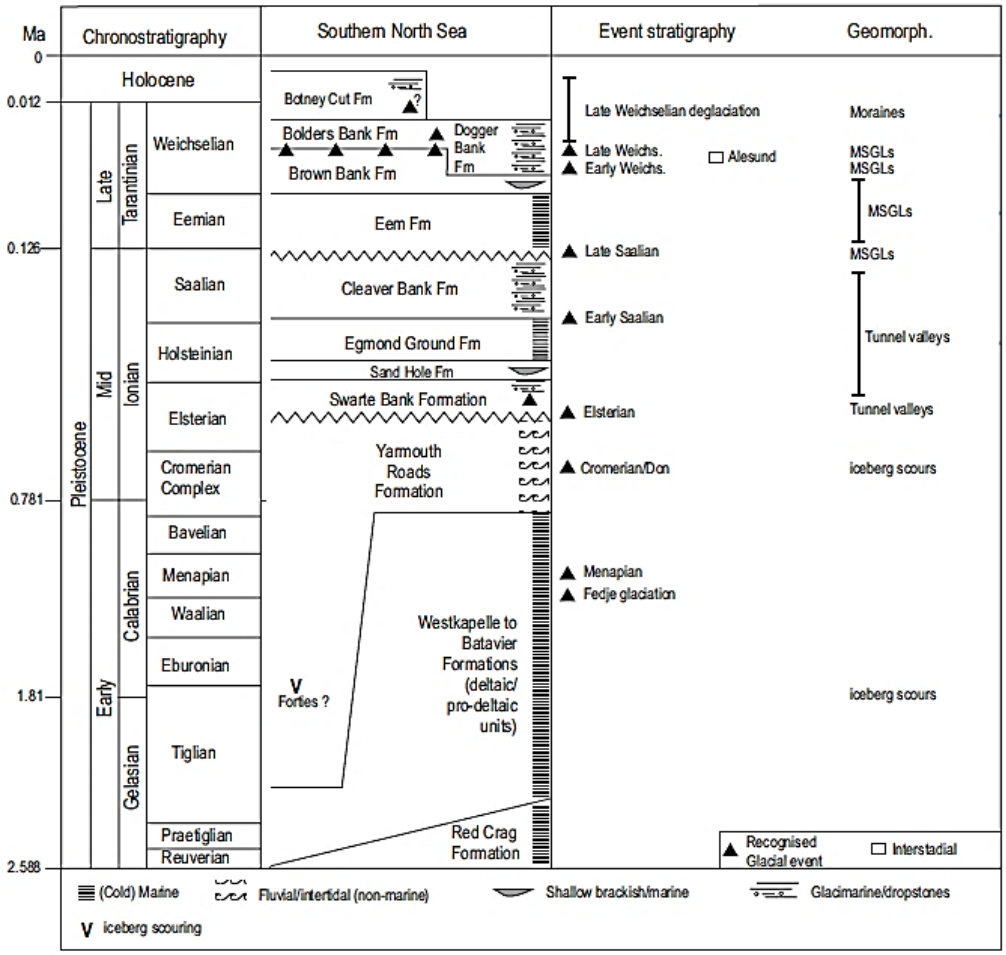

Figure 16. Diagram summarizing the stratigraphic range of the Pleistocene facies units the Southern North Sea (adapted from Graham et al., 2011).

3.2 Seismic Data Acquisition

The seismic data acquisition was carried on board of MV Bibby Tethra vessel in the Hornsea Project One Offshore wind farm, East of England, North Sea. The 3D multi-channel spread operation was carried out by GeoMarine Survey Systems and the onboard data QC/QA by *Geosurveys*.

3.2.1 Acquisition geometry

The streamers were balanced for a slanted configuration, with the tail at approximately 1 m and the head until 30 cm below surface. The following image describes the adopted 3D acquisition geometry (Figure 17).

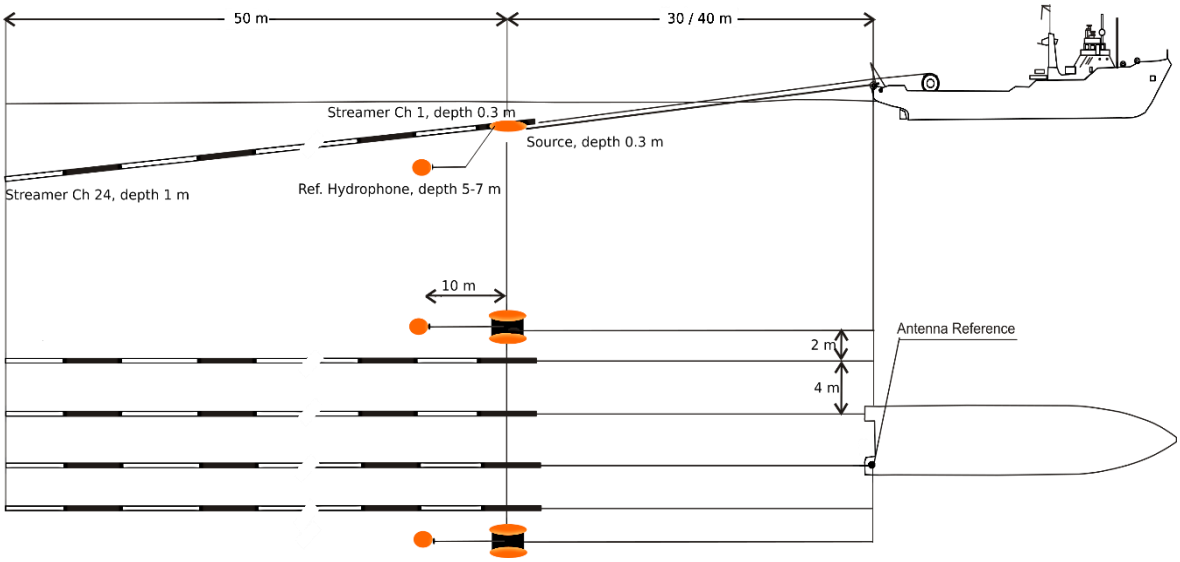

Figure 17. Acquisition Geometry scheme used in the HOW01 seismic survey.

3.2.2 Acquisition parameters

The acquisition parameters can be seen in Table 1.

Table 1. Acquisition parameters of the HOW01 survey.

Seismic source	*2x 200 LW tips Sparker*
Source Deck Lead	*30 m / 40 m*
SP Interval	*200 / 175 ms*
Operating Power	*500 J*
Power Supply	*2x Geo-Spark 2000x*
Streamer	*4x 24 Channel single element light weight streamer;*
Group Interval	*CH 1 to 12 @ 1 m, CH 13 to 24 @ 2 m*
Source Towing Depth	*0.3 m*
Ref. Hydrophone	*2x Single element Ref. hydrophone*
Acquisition recorders	*4x Multitrace 24 recorder unit; 1x Multitrace Dual Channel*
Sample Rate	*0.1 ms*
Record Length	*200 / 150 msec*
Positioning	*10x wifi DGPS beacons*

3.3 3D Seismic Blocks

During the acquisition, a 2 m *bin* grid for each volume was created in order to assign Inline and Crossline values to the volumes. The 3D seismic blocks had some problems during the acquisition, namely the gaps in the seismic (Figure 18). A possible solution to solve the problem it is the *Flex Binning* method which will be explained in the following sub-chapters since its application is one of the main goals of this thesis.

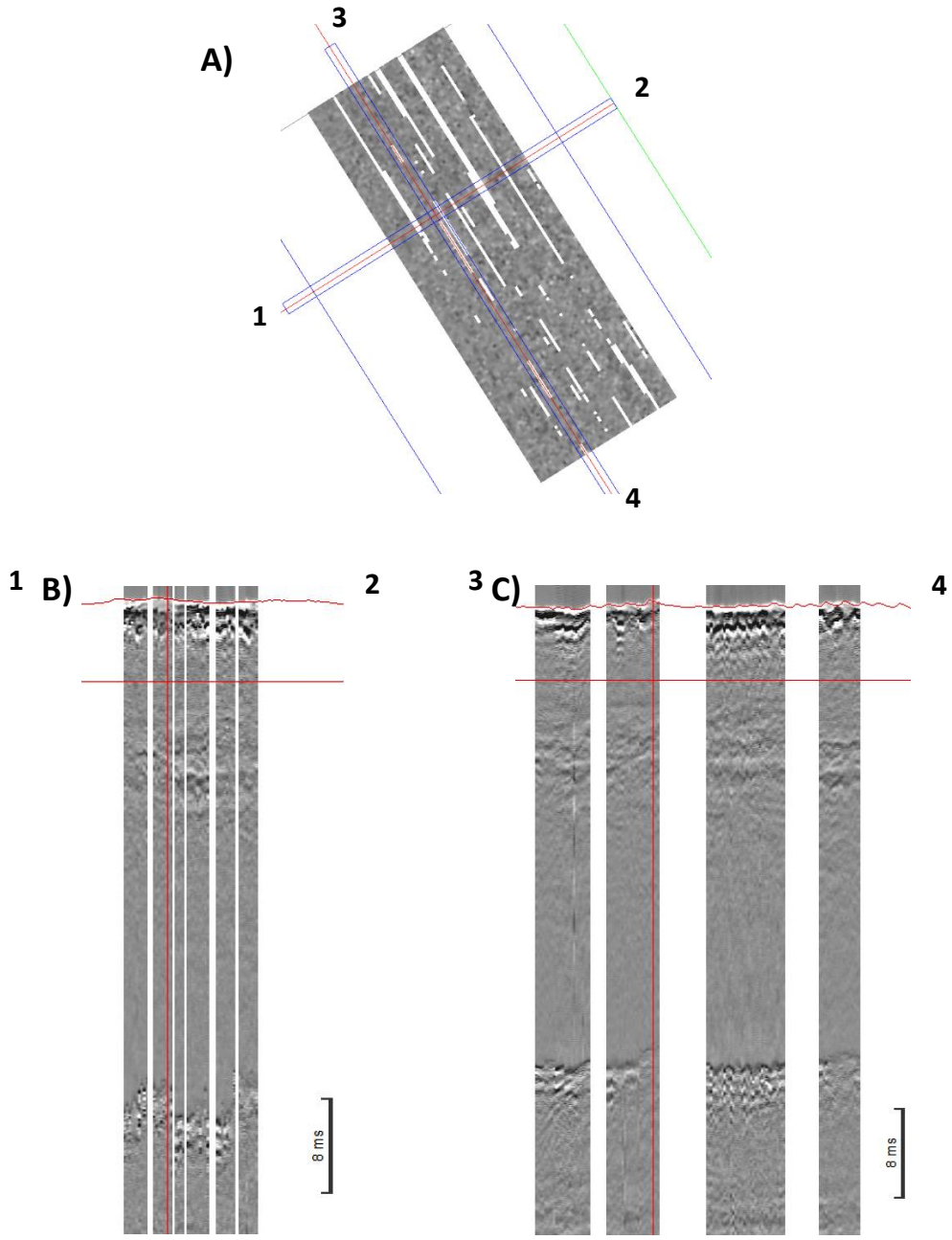

Figure 18. An example of 3D block portion where is evident the presence of data gaps, before the apply *Flex Binning*. A) Time slice display. B) Display of an XLine 1-2. C) Display of an ILine 3-4.

The area under study is also geologically highly complex, as described above in the subchapter Geological Framework of the Southern North Sea. Nevertheless, it is likely that the HOW01 UHRS data images only show the Quaternary geology. The Hornsea Offshore Windfarm Project One area was under the influence of glaciers and that is registered in its geological record (Figure 19). Also, the numerous erosional surfaces present are likely to be related with glaciers and sea level changes (Figure 19 and Figure 20).

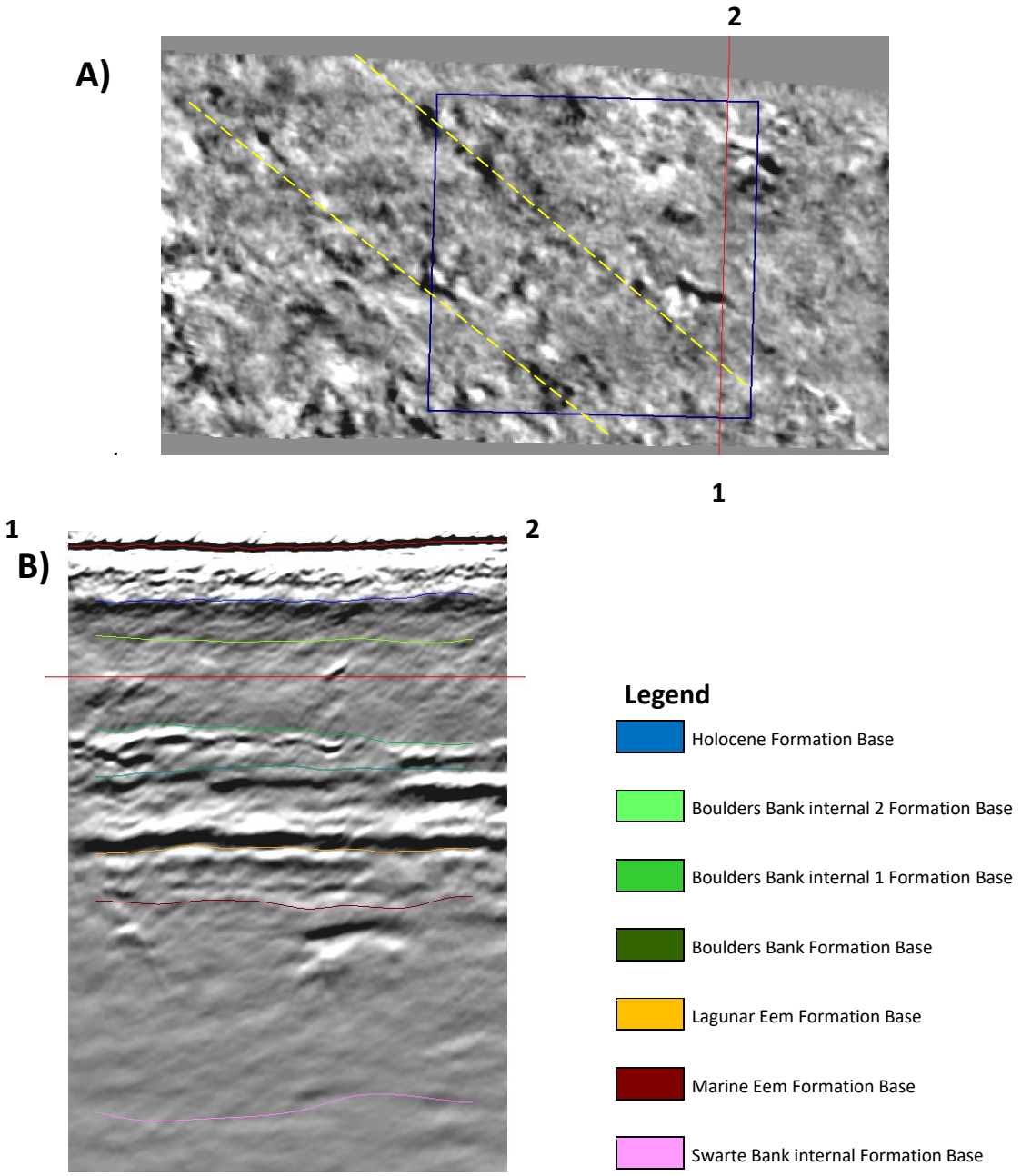

Figure 19. Seismic interpretation of the A32A31 volume. A) Depth slice display a small part of the volume A32A31, the blue square represents a Wind Tur*bin*e Generators and the lines in yellow represent the movement of the glaciers. B) XLIne display with some formation bases interpreted.

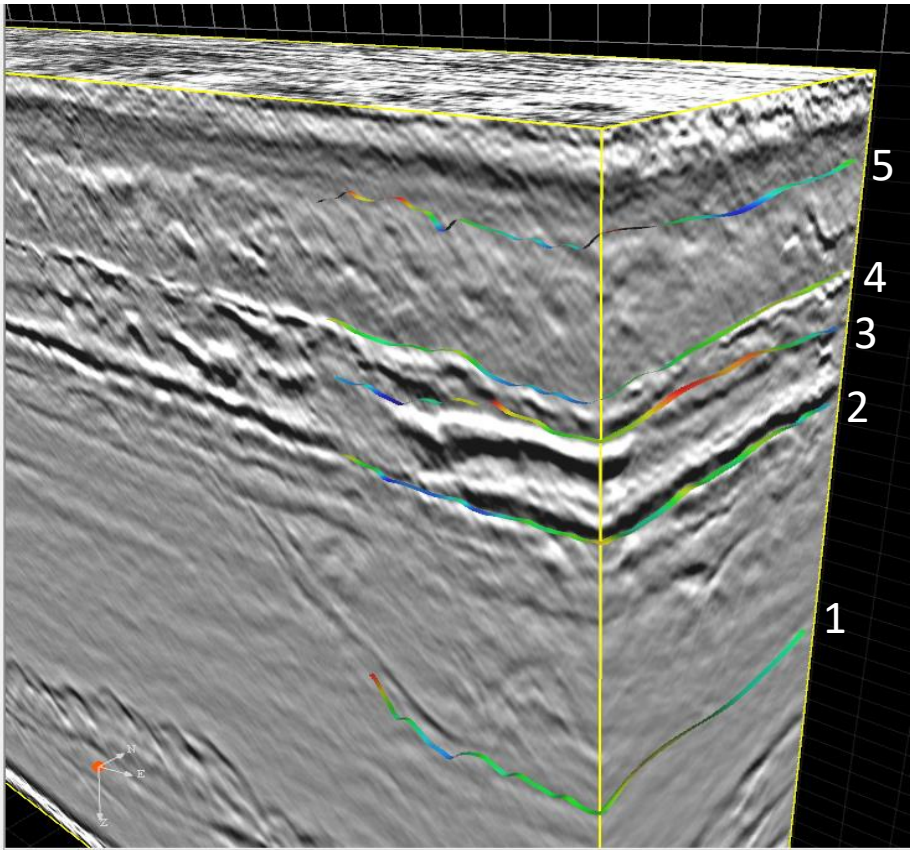

Figure 20. 3D display of the A32A31 volume with seismic interpretation. Legend: 1- Swarte Bank internal Formation Base; 2- Eem Formation Base; 3- Boulders Bank Formation Base; 4- Boulders Bank internal 1 Formation Base; 5- Boulders Bank internal 2 Formation Base.

The seismic data is recorded using a proprietary *bin*ary format. Data can be converted to SEG-Y or SEG-D format immediately after the end of the line. In a typical 3D acquisition situation, for each trace there exist at least 26 trace headers and normally 5 traces are acquired per second with 96 channels in total (4 streamers x 24 channels); after one minute of acquisition there are 28800 traces. Therefore, in an hour of acquisition there are 1728000 traces and 10368000 trace headers total.

The B27H27 seismic block took approximately 41 hours to be acquired and has 74059656 traces and 1925551056 headers. This seismic block is not the largest that *Geosurveys* has acquired, but it is possible already to see that these acquisitions involve a very large volume of traces as well as trace headers. The SEG Y files in this type of seismic datasets therefore contain a large number of traces; there are more traces than the expected in a normal dataset, which leads to *software* limitations, as SPW is not prepared for these data sizes yet. Therefore, the high dimensions of traces and headers on the dataset can be a problem, because they influence the performance of the SPW program (*software* limit), the computer *hardware* limits, and time for efficient processing.

4. *Flex Binning* Implementation in SPW

In this Chapter, after a brief explanation about *Flex Binning* and a description of the way in which it was originally implemented in SPW, the tests of its application to 3D UHRS data are described, together with the problems found and the solutions adopted.

4.1 What is *Flex Binning*?

Due to sea conditions, which often cause cable feathering, the majority of 3D marine seismic surveys do not have a regular sampling of offsets. This results in fold variation, mainly for larger offsets, or even in areas with no data at all, causing severe impacts in several steps of the data processing such as velocity analysis, multiple attenuation, stacking and migration. Surveys which have this common problem require the insertion of the *Flex Binning* method into the workflow, which is the aim of this work.

The *Flex Binning* process attempts to maintain a uniform CDP fold and offset distribution throughout the surveyed area. In order to make the distribution of offsets more uniform, the *bins* are extended by a percentage of their size *(GeoSurveys, 2016).* This extension can be made in both in-line and cross-line directions. If no trace is found within the original *bin* then a trace inside the extended *bin* is used. If several traces are found in the neighboring *bins*, usually the selected the trace is the one nearer to the *bin* centre. Figure 21 shows the process of *bin* expansion.

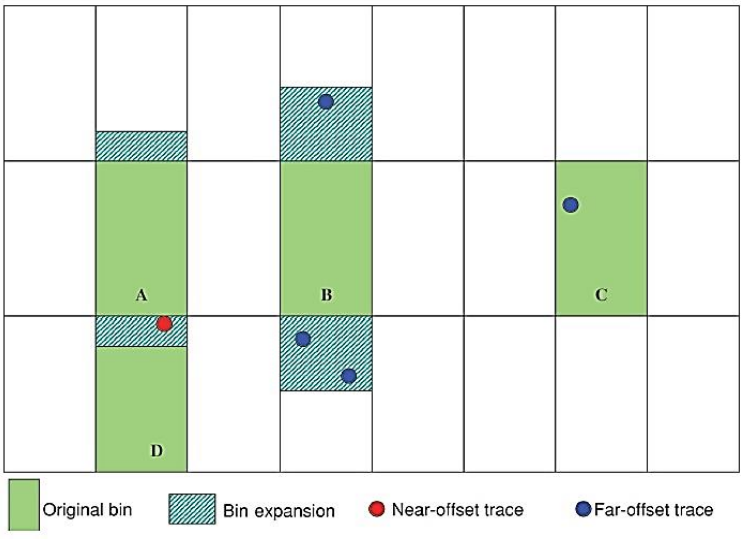

Figure 21. *Bin* expansion diagram. See text for explanation.

In Figure 21, the *bin* A is expanded for a near offset trace with a relatively small expansion. The *bin* B is searching for traces with a larger offset, i.e. with a larger *bin* expansion, and gets three results; the trace closest to the *bin centre* is the one that is borrowed. *Bin* C already has a far offset trace and no *bin* extension is needed. The red trace (near-offset trace) will end up being used by both *bin* A and D.

There are other alternative solutions, instead using the *Flex Binning*, namely the Regularization and Interpolation. In this work, the *Flex Binning* method will be used.

4.2 The SPW *Flex Binning*

As stated above, one of the main objectives of this thesis was to test the application of the available *Flex Binning* routines in the SPW *software* (from Parallel Geoscience) to Ultra High Resolution 3D seismic Datasets commonly acquired by *Geosurveys* and to investigate how to make it efficient enough so that it can be applied in the field, just after the data acquisition to fill identified cover gaps before preliminary field processing. This work was carried out in close collaboration with the Parallel Geoscience *software* development team, so that when problems were identified, solutions could be sought, implemented and new tests performed for checking the proposed solutions. For this purpose, two seismic datasets were used: (1) a medium size dataset (209 GB) and a large volume dataset (462 GB). The first one was used to detect any *software* bugs and problems before testing the *software* in a large dataset. After most of the code problems were solved, it was used the largest dataset acquired in the survey area (751 GB).

In SPW, the *Flex Binning* Processing Step consists of 2 main flows: (a) the **CMP *Binning* flow**, described in Section 4.2.2 and (b) the ***Bin* Fold Limit flow**, described in Section 4.2.3.

4.2.1 Data input

Before running the *Flex Binning* flow, just after acquisition, it is fundamental to verify first the contents in the various header positions in the SEG-Y input file, so as to create a SEG-Y format template (Figure 22) in SPW, which will be used to build the index file. SPW already has a SEG-Y standard format template, but it is often necessary to change some header values stored in non-standard positions. This was the case for the medium size dataset used in this work, because it

was retrieved after preliminary processing with the *RadEx Pro software*, which changed the byte locations of the inline and crossline, CMP Easting and CMP northing (these had to be corrected and are highlighted by the red rectangles in Figure 22) The medium size dataset has 7978 inlines and 117 crosslines.

In a new phase of the tests, it was used larger input file which came directly from the seismic data acquisition (B27H27 seismic block with 462 GB). This large size dataset has 771366 number of records, which corresponds to the number of shots; 192 traces per record which corresponds to the number of channels / receivers for each shot - since there are two seismic sources, 96 channels*2 sources=192; 1500 the samples per trace; and 0.100 ms the sample interval.

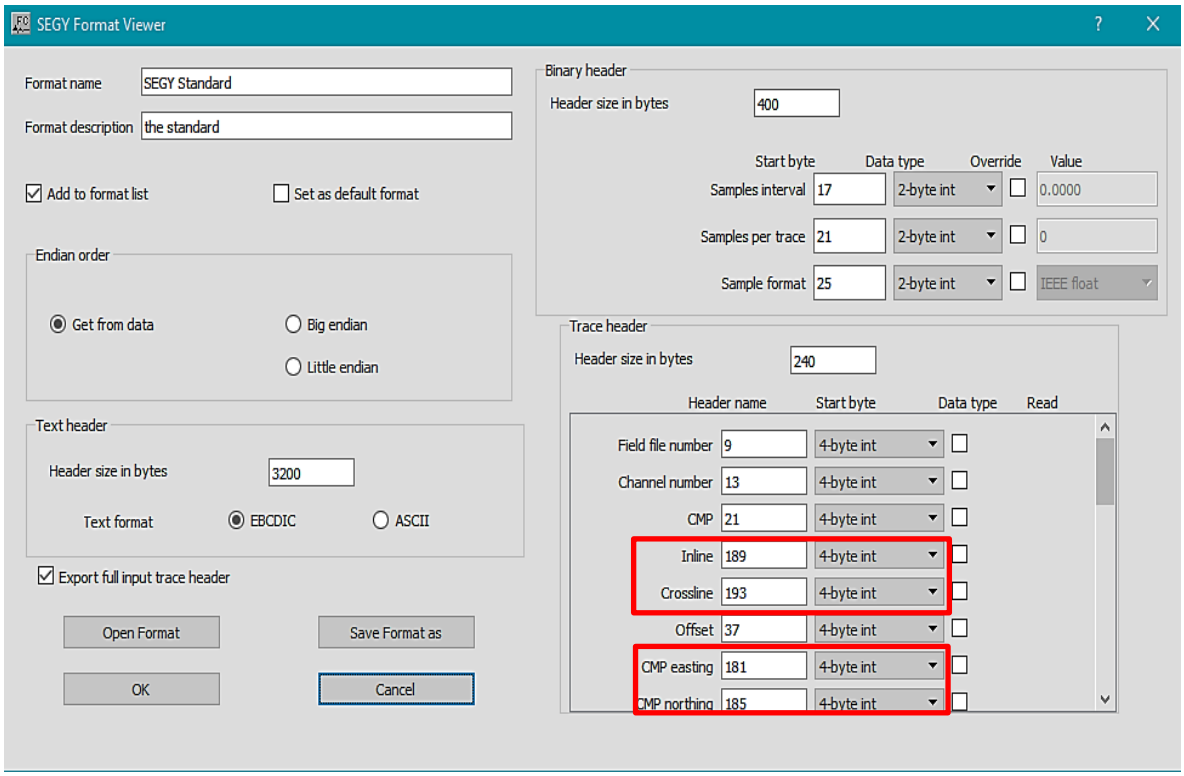

Figure 22. SEG-Y Template in SPW for the medium size seismic dataset, after correction of the header values to their standard byte location, since these had been swapped in the output SEG-Y file from the *RadEx Pro software*.

4.2.2 CMP *Binning* Flow with *Flex Binning*

The CMP *Binning* process in SPW assigns CMP line and location numbers according to user specified coordinate parameters. If a 2D survey is specified, the user is prompted to define the line. If a 3D survey is specified, the user will be prompted to define the grid.

The option of *Flex Binning* allows each *bin* to contain more traces, by increasing the effective size of each *bin* and by including traces which fall into neighboring *bins*. The amount of *Flex* can also be proportional to the trace offset. The *Flex* traces may be added immediately to the output data flow, or else their locations can be written into a *Flex* file. This option allows stacking the *Flex* traces without extra sorting.

The CMP Binning flow is composed of an Input file (seismic data in any sort order), the CMP *Binning* processing step, a CMP *Flex* Locations card and an Output file with any sort order (Figure 23).

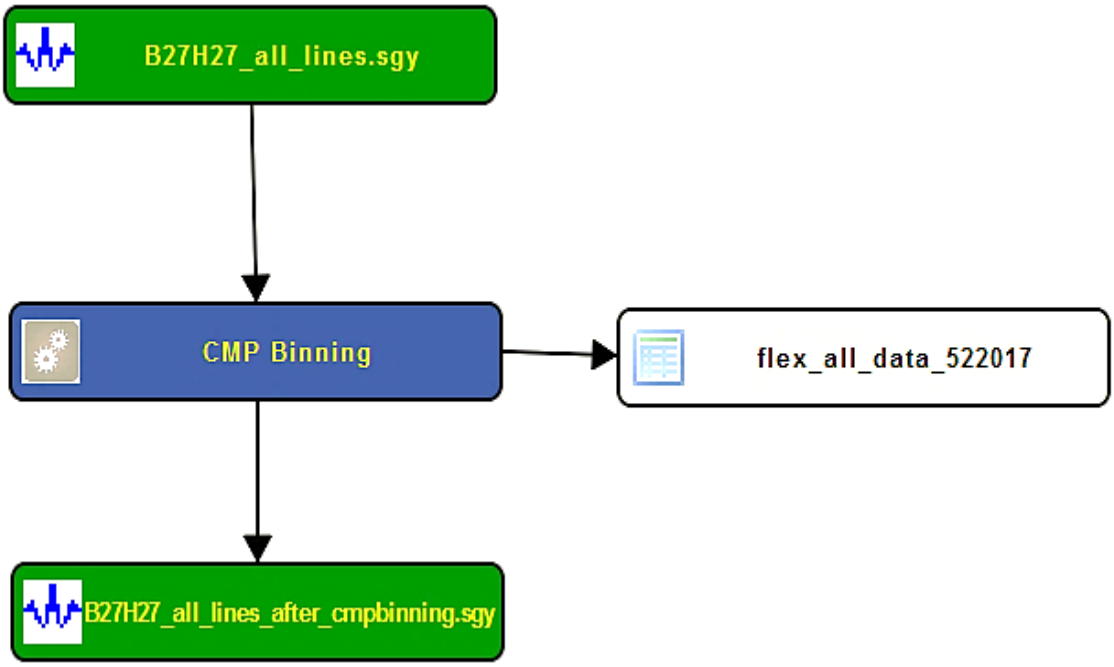

Figure 23. Example CMP *Binning* Flowchart

Input File

The input seismic file for the first tests with the medium size dataset after corrections to the header values is shown in Figure 24, where we can observe: the number of records (363244), which corresponds to the number of shots; the traces per record (192) which corresponds to the number of channels / receivers for each shot - since there are two seismic sources, 96 channels*2 sources=192; the number of traces (33556726); the samples per trace (1500); and the sample interval (0.1000ms).

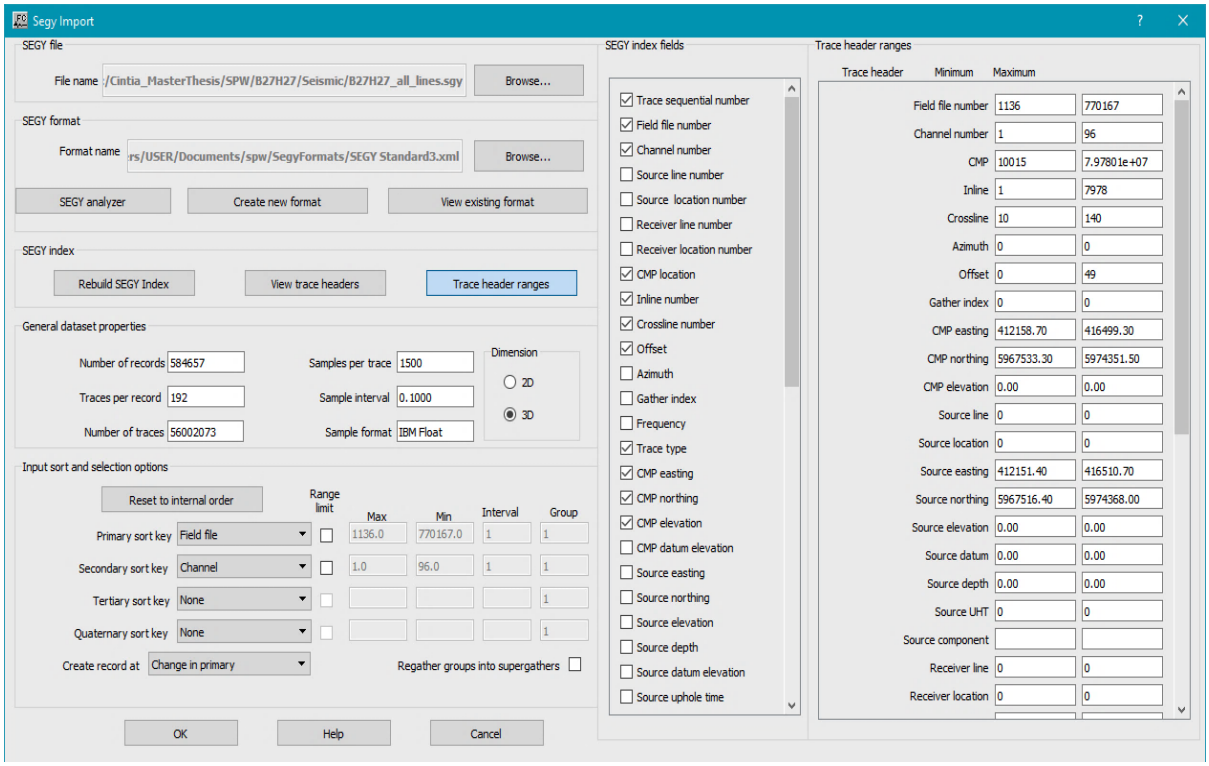

Figure 24. SEG Y Input for CMP *Binning* flow with the medium size dataset.

CMP Binning Processing Step

To implement the CMP *Binning* step, it is necessary to fill in the parameters inside the CMP Binning window shown in Figure 25. The parameters are: grid definition, coordinate definition, survey dimensions, project updates, *Binning* type specification, *Flex Binning* specification and input header coordinates. The coordinates of the grid (3D survey area) are inserted by defining three of its corners, which are:

- **Corner 1 Easting:** Enter the easting (x) coordinate of the first corner of the survey.
- **Corner 1 Northing:** Enter the northing (y) coordinate of the first corner of the survey.
- **Corner 2 Easting:** Enter the easting (x) coordinate of the second corner of the survey.
- **Corner 2 Northing:** Enter the northing (y) coordinate of the second corner of the survey
- **Corner 3 Easting:** Enter the easting (x) coordinate of the third corner of the survey.
- **Corner 3 Northing:** Enter the northing (y) coordinate of the third corner of the survey.

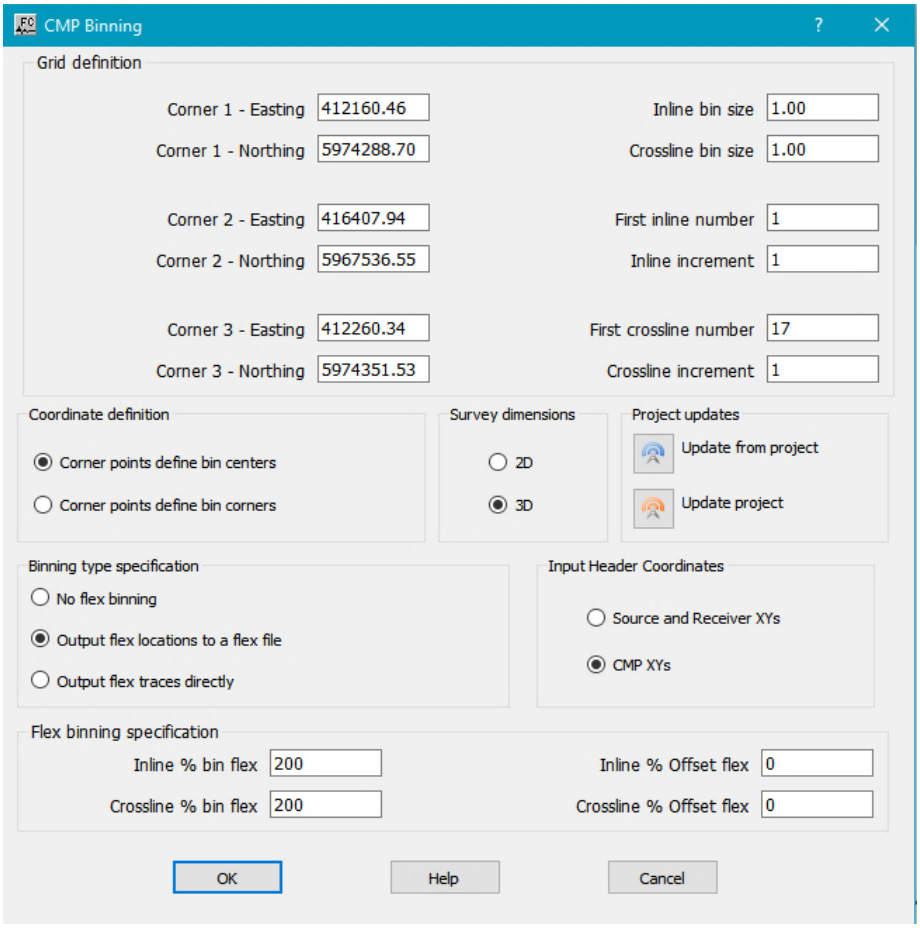

Figure 25. Step parameters for the CMP *Binning* window

For the grid definition, it is essential also to insert:

- the **Inline *bin* size:** Enter the size in distance units of the inline side of each *bin*.
- the **Crossline *bin* size:** Enter the size in distance units of the crossline side of each *bin*.
- the **First inline number**: Enter the first inline number. This line number is assigned to all the *bins* along the side of the survey from corner 1 to corner 2.
- the **Inline increment**: Enter the increment in line numbers between adjacent CMP lines.
- **First crossline number**: Enter the first crossline number. This location number is assigned to all the *bins* along the side of the survey from corner 1 to corner 3.
- the **Crossline increment**: Enter the increment in locations between adjacent CMP locations.

The coordinate definition, specifies whether the corner points define the *bin* centres or corners, explicitly:

- **Corner points define *bin* centres**: Select to specify that corner points define *bin* centres. It is used this coordinate definition (Figure 26).
- **Corner points define *bin* corners**: Select to specify that corner points define *bin* corners.

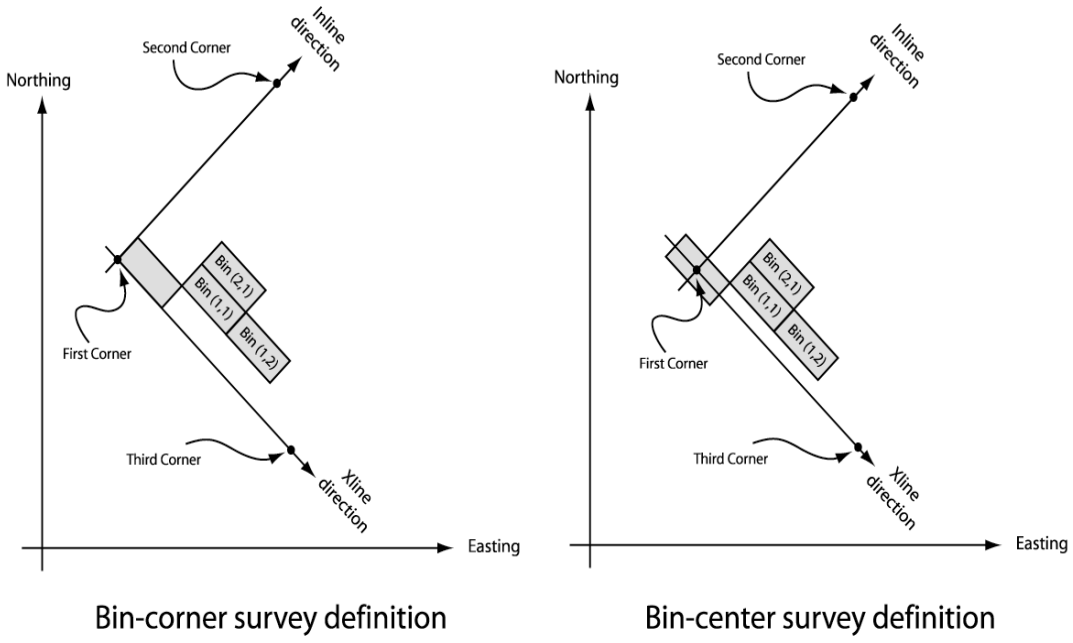

Figure 26. Coordinate definition in SPW.

The survey dimensions need also to be specified both for 2D and 3D, namely:

- **2D**: Select to specify 2D line survey dimensions.
- **3D**: Select to specify 3D grid survey dimensions (the case of this work).
-

In SPW it is possible to make updates from the project:

- **Update from project**: Select to update from the project.
- **Update project**: Select to update the project.

The *Binning* type specification, can be as follows:

- **No *Flex Binning***: Select standard *Binning*, with no extra traces added.
- **Output *Flex* traces directly**: Select to add *Flex* traces to the output *bin*ned traces.
- **Output *Flex* locations to a *Flex* file**: Select to add the locations of *Flex* traces to an additional output *Flex* file. This is the way to get an output *Flex* location that is going to be used for *Flex* data, in *Bin* Fold Limit.

The input header coordinates were implemented when SPW version 2 was released and were improved in version 3. With the input header coordinates it is possible to specify whether the Header coordinates of the input are Source and Receiver XYs or CMP XYs and Offset:

- **Source and Receiver XYs:** Select to specify that the trace midpoint position and trace offset will both be calculated from the Source Easting and Northing and the Receiver Easting and Northing trace headers.
- **CMP XYs and Offset**: Select to specify that trace midpoint position will be taken from the trace headers CMP Easting and CMP Northing, and the offset will be taken from the offset header.

The *Flex Binning* specification (Figure 27) allows choosing the standard *Binning* or the type of *Flex Binning* required:

- **Inline % *bin Flex*:** Specify the percentage increase of each *bin* size in the inline direction to include extra '*Flex*' traces.
- **Crossline % *bin Flex*:** Specify the percentage increase of each *bin* size in the crossline direction to include extra '*Flex*' traces.
- **Inline % Offset *Flex*:** Specify the increase of each *bin* size as the percentage increase of the trace inline offsets.
- **Crossline % Offset *Flex*:** Specify the increase of each *bin* size as the percentage increase of the trace crossline offsets.

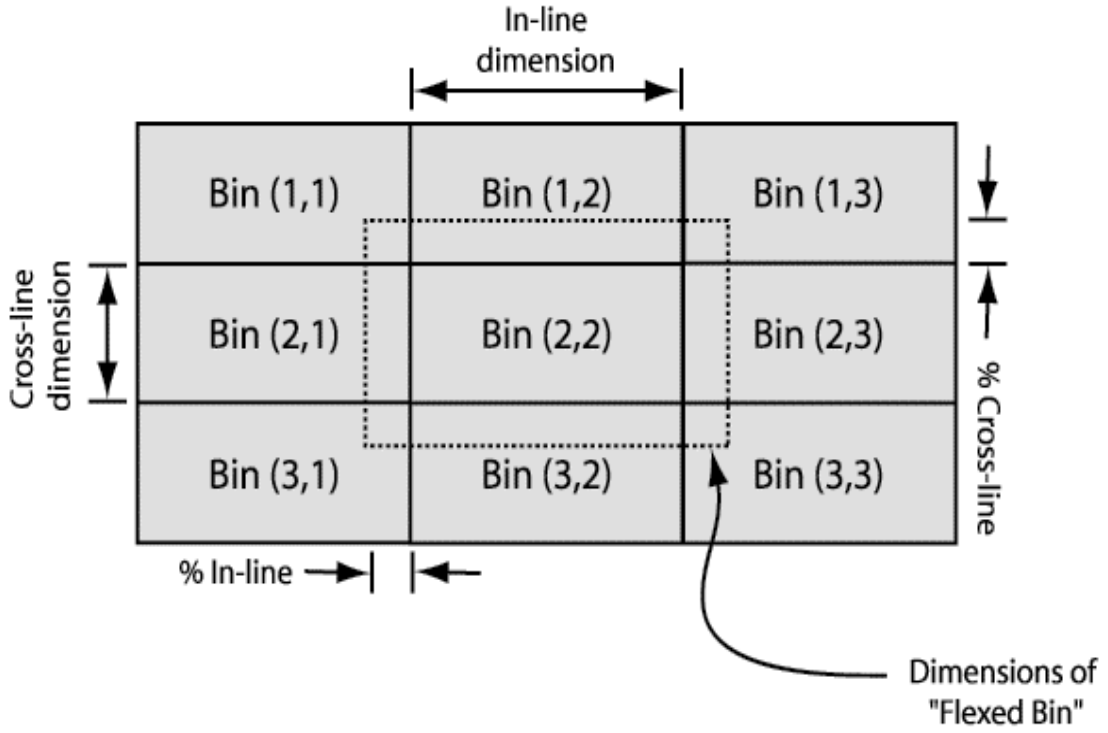

Figure 27. Diagram representing how % *Flex* works on the data.

The *Flex Bin*nig is done in the CMP domain. The mid-point of every trace from a shot to a receiver is assigned to the CMP *bin* which contains that mid-point. The *bins* making up the survey area are all rectangular. With *Flex Binning*, each *bin* is larger than the standard non-*Flex bin* size. A 20 % - 20 % *bin Flex* means that the length of each *bin* (in-line size) and the width of each *bin* (cross-line size) are 20% longer each than the standard *bin* length and width.

Therefore, if the standard *bin* size is 1m X 1m, 100% *Flex* would be taken as meaning the *Flex bin* size is 2m X 2m (i.e. increased by 100%). The distance to each of the *bin* boundary lines from the *bin* centre, would have increased from 0.5m to 1m. Each trace in this case can be expected to land in four different *bins* – one being its standard nearest non-*Flex bin*, and the other three in neighboring *Flex-bins*. This of course depends on whether the trace mid-point falls in the centre or near the edge of the survey. In the case of a % *Flex* in each direction which is not a multiple of 100%, or if the in-line and cross-line *Flex* %s are different, the number of *Flex bins* that a trace falls into will vary depending on its exact location.

Output File

The output CMP *bin*ned dataset will contain only the original traces which fall within the survey area if you set to drop out dead traces and already had the grid implemented according to the parameters established by CMP *Binning* card. It won't contain *Flex* traces. The output seismic file from the CMP *Binning* flow appears with trace headers Inline and Crossline, in the same position of the CMP Line Location and CMP Location, respectively.

CMP *Flex* Location Output Card (*Flex* Table)

The *Flex* table is filled in by the *Flex* locations from the 3D dataset. Although it was suggested that this output file should be in a text format, this has not yet been accomplished by the *software* development team and the output *Flex* Table is still at present in an image format. Thanks to some of the suggestions proposed it is nevertheless now possible to open the CMP *Flex* Locations dialog box and see how the file has been filled in (Figure 28). It is also now possible to save the *Flex* file location in a *Flex* File format, but again not yet in a table format.

The *Flex* table parameters that can be checked are:

- **Currents Records:** Lowest and highest input trace numbers (ID), and the ranges of CMP lines and locations (first and the last CMP lines/ CMP locations) written should be stored in the file header.

- ***Flex Binning* Specification:** Write the specification that was stable before in the CMP *Binning* step (Inline % *bin Flex*, Crossline % *bin Flex*, Inline % Offset *Flex* and Crossline % Offset *Flex*).

Two further options that were requested and are now available in the latest *software* version, are:

- **"Append to existing dataset"**: to continue adding *Flex* locations to the specified *Flex* file. Otherwise if the specified *Flex* file exists it will be renamed with the addition of suffix'_copy' and a new file of the specified name opened.

- **"Scan File":** to read through the file and check that the reported record statistics are correct. Warning: for large files this process can take considerable time.

When the CMP *Binning* flowchart is run, the CMP *Flex* Location cart is filled with Current Records and *Flex Binning* Specification.

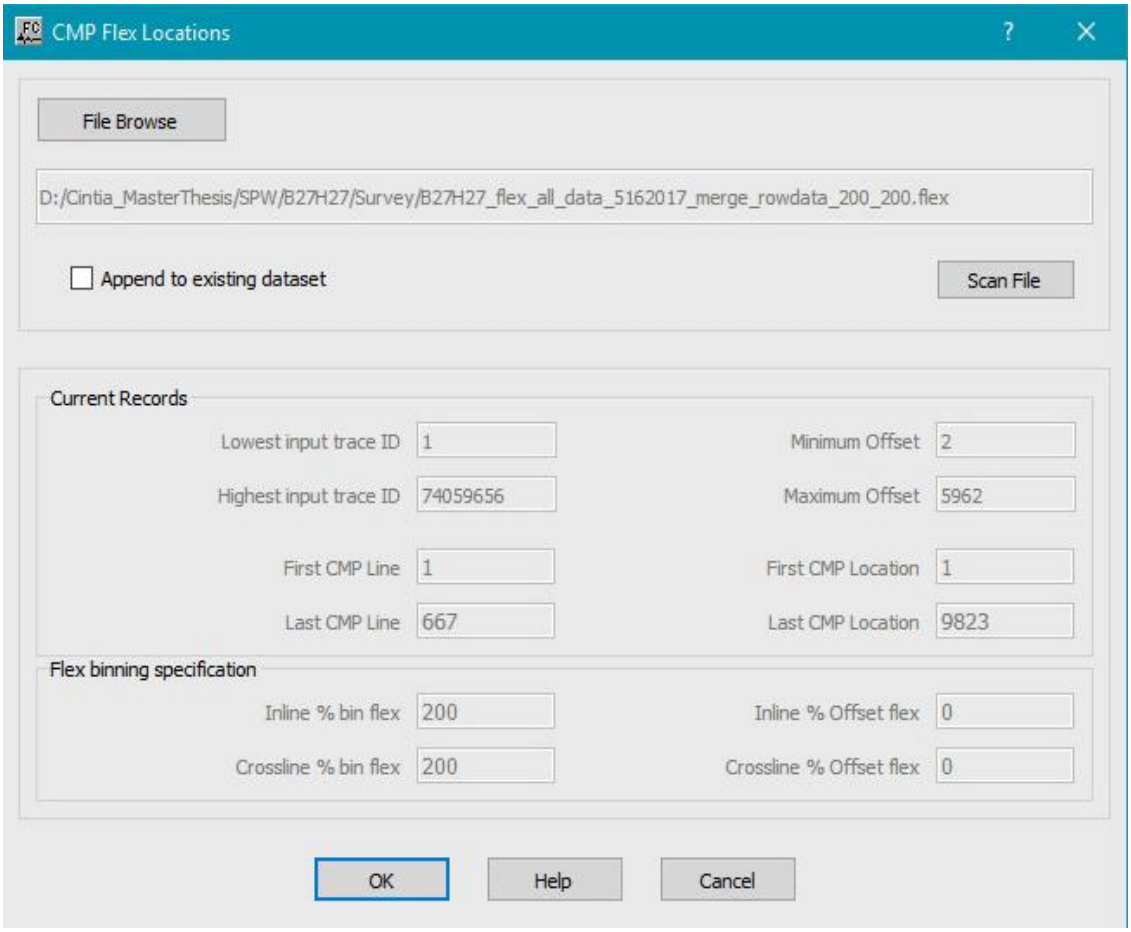

Figure 28. CMP *Flex* Location dialog window.

4.2.3 *Bin Fold Limit Flow*

The *Bin* Fold Limit Flow (Figure 29) adds extra *Flex* traces to the input binned data from an input *Flex* table. The *Flex* traces are selected from the *Flex* table locations as specified by the *Bin* Fold Limit parameters. The output is the 3D Seismic data sorted by CMP Line and CMP Location. The input parameters are:

1) 3D Seismic data sorted by CMP Line and CMP Location, with CMP Location as the record key (mandatory).
2) A *Flex* Table generated as the output of CMP *Binning*, with *Flex* trace location data.

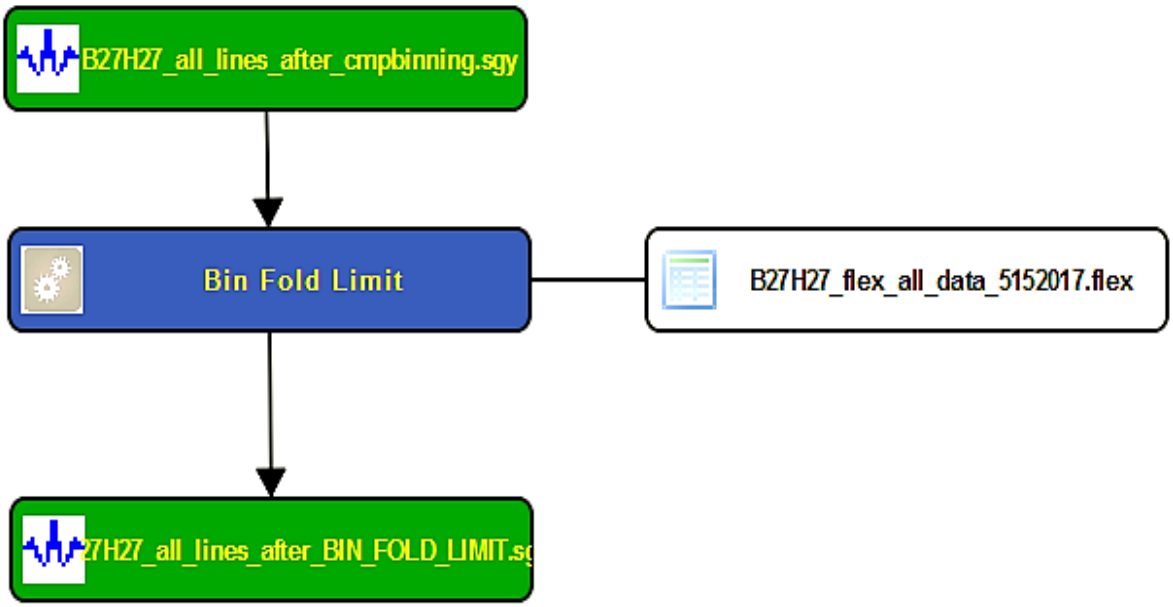

Figure 29. Example *Bin* Fold Limit Flowchart. See text for further details.

Figure 30 shows the dialog box for the *Bin* Fold Limit processing step.

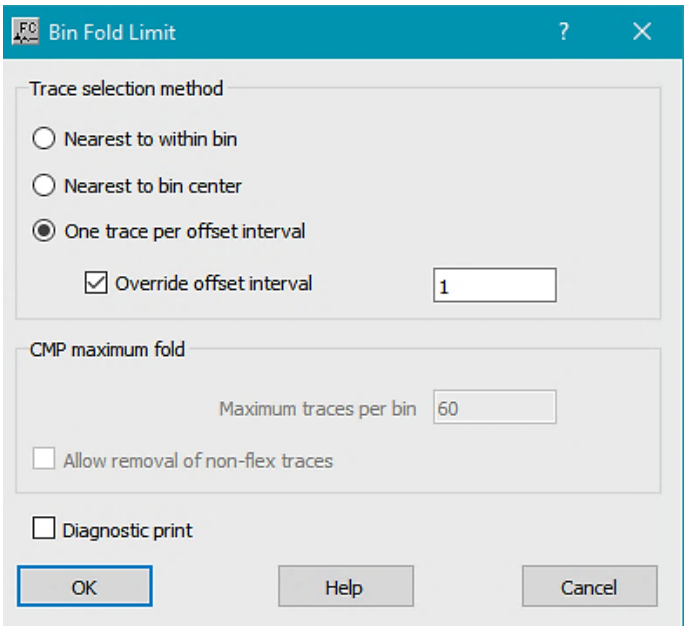

Figure 30. Dialog box for the *Bin* Fold Limit.

Trace selection Method: The trace selection method specifies the criterion by which traces are selected from both the input data and the *Flex* traces.

- **Nearest to within *bin***: Select to specify that the traces selected for each *bin* will be those within the *bin* plus those closest to the *bin* boundary, subject to the specified maximum fold. If removal of non-*Flex* traces (i.e. Those within the *bin*) is allowed, the traces selected will be those closest to the *bin centre*. If checked, traces will be selected for inclusion in a *bin* by their distances from the *bin* boundary.

- **Nearest to *bin* centre**: Select to specify that the traces selected for each *bin* will be those within the *bin* plus those closest to the *bin centre*, subject to the specified maximum fold. If removal of non-*Flex* traces (i.e. Those within the *bin*) is allowed, the traces selected will be those closest to the *bin centre*. If checked, traces will be selected for inclusion in a *bin* by their distances from the centre of the *bin*.

- **One trace per offset interval**: This option aims to provide a full range of offsets within each *bin* by allowing just one trace per offset interval. This option can be overridden, if necessary, using **Override offset interval** and selecting the desired number of traces per offset interval.

The CMP maximum fold: this does not apply when traces are selected for inclusion in a *bin* of one trace per offset interval. Otherwise, it is possible to choose:

- **Maximum traces per *bin***: Specify the total number of traces that may be included in each *bin*.

- **Allow removal of non-*Flex* traces**: If checked, and there are more (non-*Flex*) traces assigned to a *bin* than the specified Maximum traces per *bin*; then, those farthest from the *bin* centre will be removed. If not checked, only *Flex* traces which fall within the box will be de-selected.

If the diagnostic print is selected, traces with mid-points within a *bin* will be removed if necessary to maintain the selected maximum fold. If not checked, these traces will not be removed, even if specified maximum fold is exceeded.

4.2.4 *Flex* coverage map

Another missing item that was requested to be implemented was a map with the *Flex* location. In the latest version however, the *Flex* location file format was changed and therefore old format *Flex* location files cannot be used anymore and only *Flex* location files created with the newer version can now be used to build the map from *Flex* File. The plotting routine used to create the Flex coverage maps is the same that was used in SPW to plot the fold coverage map. If the offset increment when plotting a fold map from a *Flex* file is not 1, it will not work, and the *software* will probably crashes. The SPW team tried to fix this, and put also reporting the offsets range on the *Flex* file dialog. This is a nice feature to have when plotting fold maps with different offsets. The new parameters of *Flex* map (Figure 31) are described below. As concerns the *Flex* Locations file, an output file from the CMP *Binning* flow with output *Flex* locations should be used.

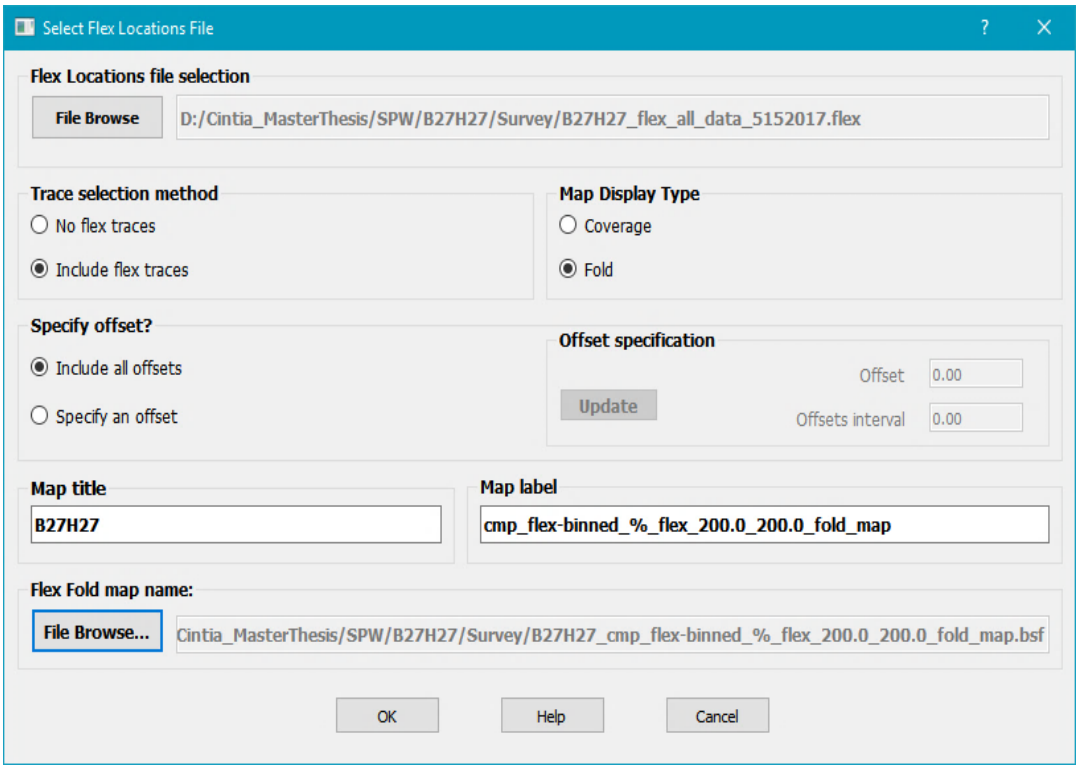

Figure 31. Dialog box to generate fold maps from a *Flex* Location File.

The trace selection method specifies whether standard binned traces (no *Flex* traces) or *Flex*-binned data (include *Flex* traces) are to be used to generate the fold map:

- **No *Flex* traces:** Select to specify that only the traces assigned to CMP *bins* without *Flex-Binning* will be included.

- **Include *Flex* traces:** Select to specify that all normally CMP-*bin*ned plus the *Flex*-*bin*ned traces will be included.

The map display type specifies whether the output map is to be a *bin*ary coverage map (1=*bin* has at least one trace), or a fold map:

- **Coverage:** Select Coverage to specify that a CMP *bin* will be given a value of 1 if at least one trace is assigned to it.
- **Fold:** Select Fold to specify that CMP *bin* will be given a value equal to the number of traces assigned to it.

The offset specification allows selecting whether to include all offsets, or just ones of a selected offsets range:

- **Include all offsets:** Select to specify that the traces at all offsets will be included in the *bins* displayed on the output map.
- **Specify an offset:** Select to specify an offset and an offset interval which will restrict the traces included in the *bins* on the output map.

The offset specification is made by the offset range for inclusion of traces.

- **Offset:** Specify the offset of trace to include in *Binning* on the output map.
- **Offset interval:** Specify the offset interval to use.
- **Update:** Specify the offset range for inclusion of traces.

The map title by default will be the project name, but the user may modify this name if required. The map label by default will be text made from the specified parameters for easy reference, but the user may modify this if required.

Unfortunately, it is not yet possible to make a fold/coverage map from a large *Flex* location file, because when we attempt to create the map from a *Flex* Locations File with 35.4 GB, the SPW closes without creating any dump file, or error message. Maybe this happens because the file is very big and the computer cannot find enough memory to allocate the map to be displayed. The size of *Flex* Locations File generated by this process was 2.37 GB and the same problem always happens. This problem still needs to be solved.

4.3 Beta testing, problems encountered and solutions adopted

In this section, the tests carried out in the scope of this work to analyze the performance of the *Flex Binning* Codes, detect problems and propose solutions are described. As stated above, these tests were first carried out on a medium size dataset to determine the main problems in the Flex routines and try to solve them, if possible avoiding too long computational times and severe memory issues (in some cases even just a portion of the medium size dataset was used for faster testing and solution implementation). Once the main issues were identified and largely solved, a new set of tests were performed in the Large Size Dataset to assess the full functionality of the application of *Flex Binning*. All the tests were performed on a Windows Workstation with an i7-6700 (3.4GHz) processor with four cores, 32GB RAM and a 1TB SSD (a high speed access disk).

4.3.1 Beta Tests of the *Flex Binning* Routines with the Medium Size dataset

During the Beta Testing of the Flex routines, several problems were encountered, both code issues and bugs. The inputs used in the Beta Testing have a large number of traces and headers, which influences the performance of the SPW, the computer *hardware* limits, and the processing time.

At the beginning of the CMP *Binning* flow tests the medium size dataset (with 209 GB) was used (see details in Section 4.2.1 and Figure 24 in Section 4.2.2). The CMP *Binning* flow did not run and the *software* crashed. The indexing of the output from the CMP *Binning* flow was not written. After many tests with numerous versions of SPW to attempt to solve this problem, the CMP *Binning* flow code was finally corrected and is now able to run without any error message and to write correctly the index output file. The total elapsed time was 8 hours, 31 minutes, 53 seconds, for a 200% *Flex Binning*. The memory used when the CMP *Binning* flow was running was approximately 40-99%. It was discovered that until 70% of the processing job, the memory used was fine (around the 50%), but after running 70% of the job, the memory usage increased significantly; for example, after 79% of the job was completed, the memory used stabilized in 98-

99% until the end (Figures 32 A and B). This high memory usage has led us to detect *hardware* problems caused by the *software* limitations.

In order to test where the problem was coming from, the same flow was run again, but without writing the output *Flex* location file; in this case, the memory used behaved very well, and did not exceed 28%-50% (Figures 33 A and B). These results obtained with the medium size dataset (209 GB) showed that the problem was related to the writing of the output file and they were sent to the SPW *software* development team to try to solve this problem.

A)

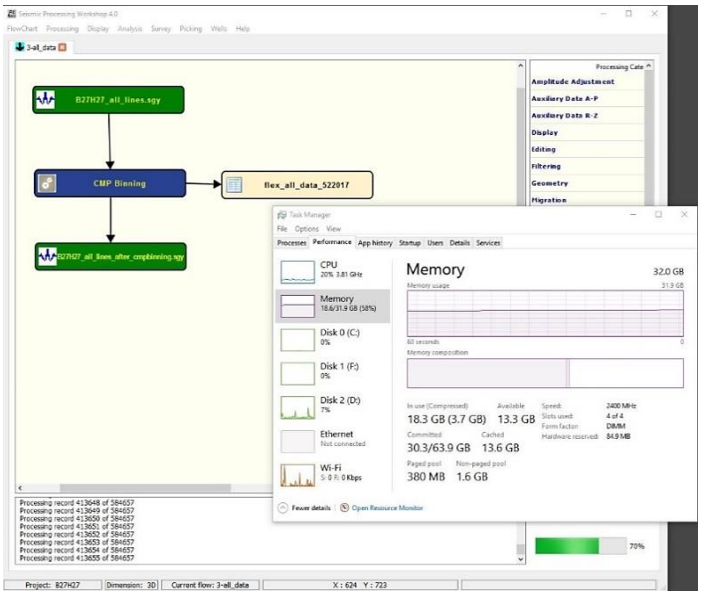

B)

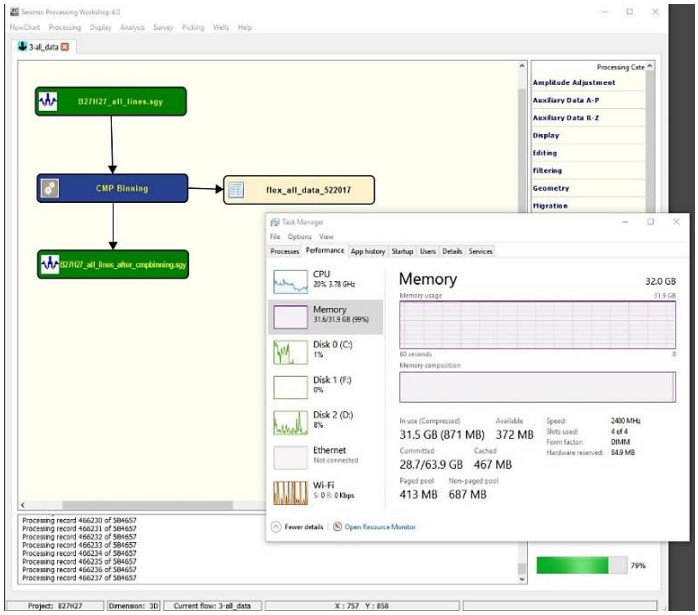

Figure 32. Memory issues when the CMP *Binning* flow with the medium size input file. A) Until 70% of the processing job, the memory was fine. B) After running 79% of the job, the memory usage suddenly increased to 99%.

A)

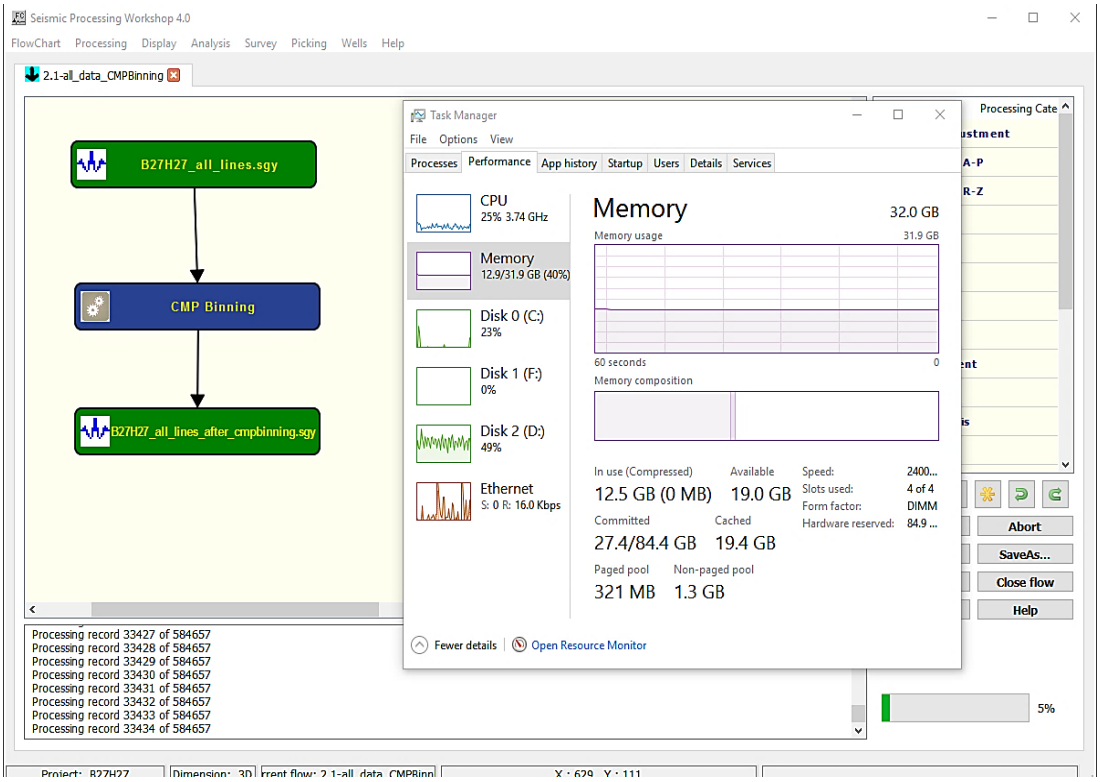

B)

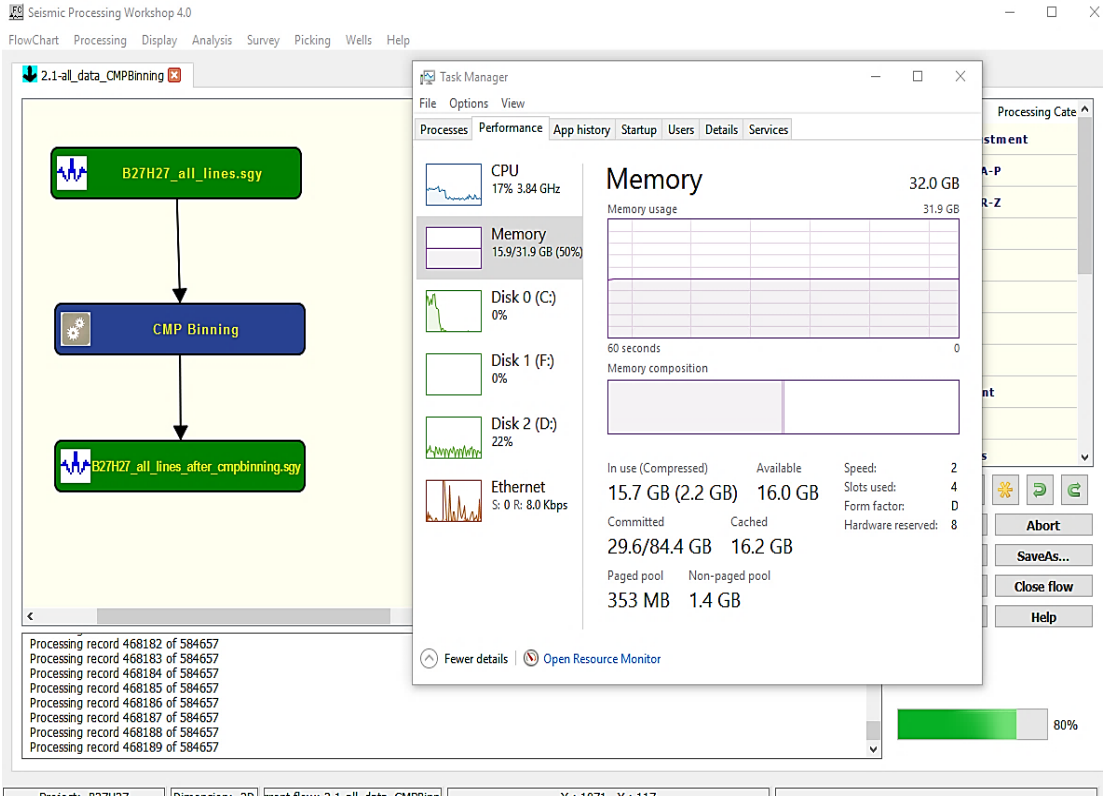

Figure 33. Memory usage when the CMP *Binning* routine was run without *Flex Binning*, i.e. without creating and output *Flex* location file.

To start realizing how the % *bin Flex* that was used could influence the time efficiency of processing, the same input was used, but with a slight change in the CMP *Binning* flow. This slight change was the % *bin Flex* chosen which was now slightly higher (250% *bin Flex* in inlines and crosslines). The total elapsed computing time was 9 hours, 17 minutes, 46 seconds. In comparison to the same job that was run with the 200% *bin Flex* in inlines and crosslines, the flow with 250% *bin Flex* in inlines and crosslines took approximately 10% more time to run when a 25% larger percentage of *bin Flex* was selected.

4.3.2 Beta Tests of the *Flex Binning* Routines with the Large Size Dataset

With the improvement of the of Flex routines code, it was then possible to move to a new phase of the tests, namely using a much larger input file which came directly from the seismic data acquisition (see details in Section 4.2.1). The input file was now 462 GB and the CMP *Binning* flow did not run and error messages appeared. The error messages that came up while processing record 1 of 5962 was "*Error: The trace header CMP Eastings and Northings header values are bad or do not conform to the survey. Correct headers or survey corners and resubmit; Processed 1 records; error writing index file trace sort list - QFileDevice Error code 0; Error while writing the index file: B27H27_after_cmpBinning.sgy*".

Therefore, in the input merged file it is necessary to first remove the bad traces. The Kill Traces step was chosen to try to solve this problem (Figure 34 and Figure 35), but it did not work.

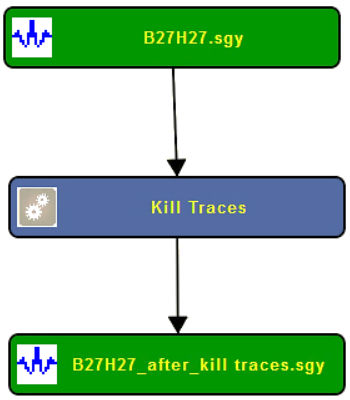

Figure 34. Experimental flow using the Kill traces step.

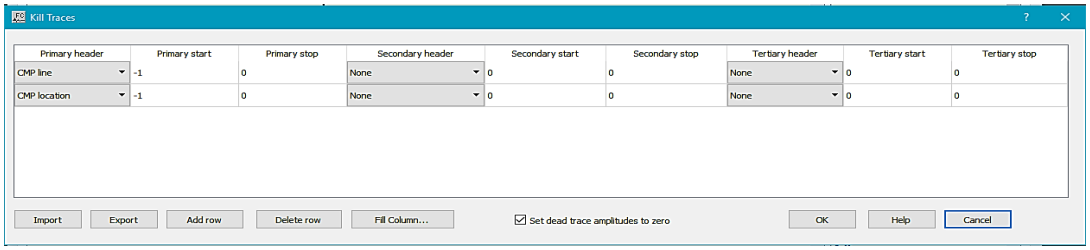

Figure 35. Experimental Kill traces card.

The solution for this problem, implemented in the SPW *software* consisted in setting the traces outside the specified area (grid), due to incorrect coordinates, as dead traces, and flag them so that these are not included in the output seismic file. After this correction, it was possible to run the CMP *Binning* flow with bad traces or traces outside the grid, but still the flow still did not work successfully.

A new error message now appears when the flow running: "***Warning: Unable to allocate memory for TraceHeadersList->ItsTraceHeaderArray in ScanSegyHeader*". This error message means that we are running out of memory for the trace header list which was used to build the index file. Solving this problem required some *software* design changes. The new updated version of SPW included changes made to the index file and now the index file is created at the end of the processing so that there will be a pause and scan of the data file before the "Processing Complete" message appears. This way, the SEG-Y output is always completed and the index which requires substantial memory is created as *a read after write* operation on the output file, without the memory failures that were happening due to the large size of the input file.

After the *software* design changes described above, the CMP *Binning* flow now runs without any error message and the program does not crash. The total running time was 14 hours, 25 minutes, 7 seconds, for 200% Flex bin and the memory usage did not exceed approximately 50% (Figure 36).

In *CMP Binning* flow the input file is generally larger than the output file, because when the CMP *Binning* is applied, a 3D grid is defined and all traces outside the selected grid are considered as dead traces and removed. As before, the same CMP *Binning* flow was run again, but in this time with a percentage of *bin Flex* of 250%. The memory used still remains quite low (Figure 37) and the total elapsed time was now 16 hours, 6 minutes and 23 seconds. In comparison to the same job that was run with the 200% *bin Flex* in inlines and crosslines, the flow with 250% *bin Flex* in inlines and crosslines took approximately 12% more time to run when a 25% larger percentage of *bin Flex* was selected, similar to the results obtained from the medium size dataset.

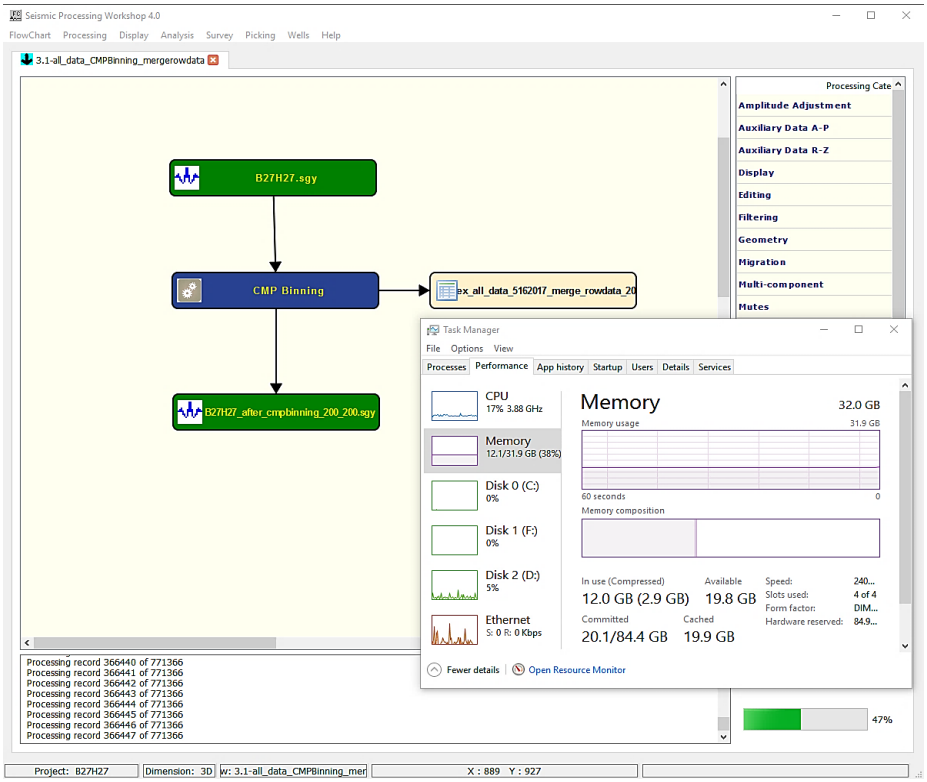

Figure 36. The memory used when CMP *Binning* was run with 200% *Bin Flex*.

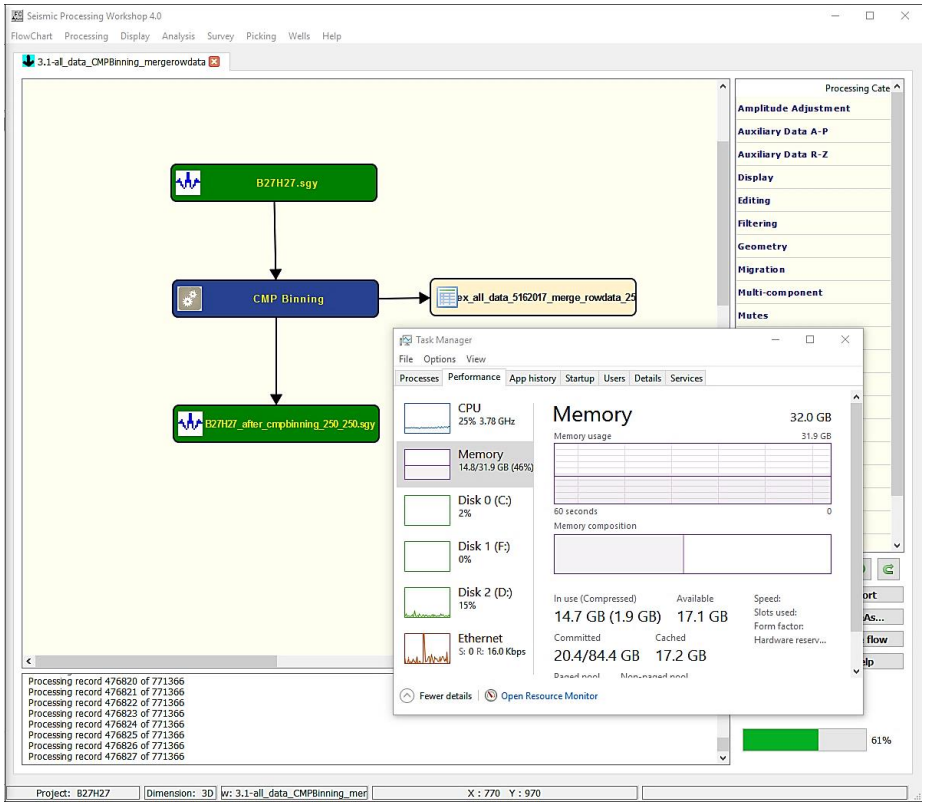

Figure 37. The memory used when CMP *Binning* was run with 250% *Bin Flex*.

In the final phase of this work, it was possible to run the CMP *Binning* flow for the largest dataset acquired in the survey area (751GB), with the final SPW version after all the testing, suggested corrections and solutions implemented. The CMP *Binning* flow was able to run without any error messages and the *software* did not crash. The total running time for this dataset was 22 hours, 26 minutes, 11 seconds. The memory usage did not also exceed 55% (Figure 38).

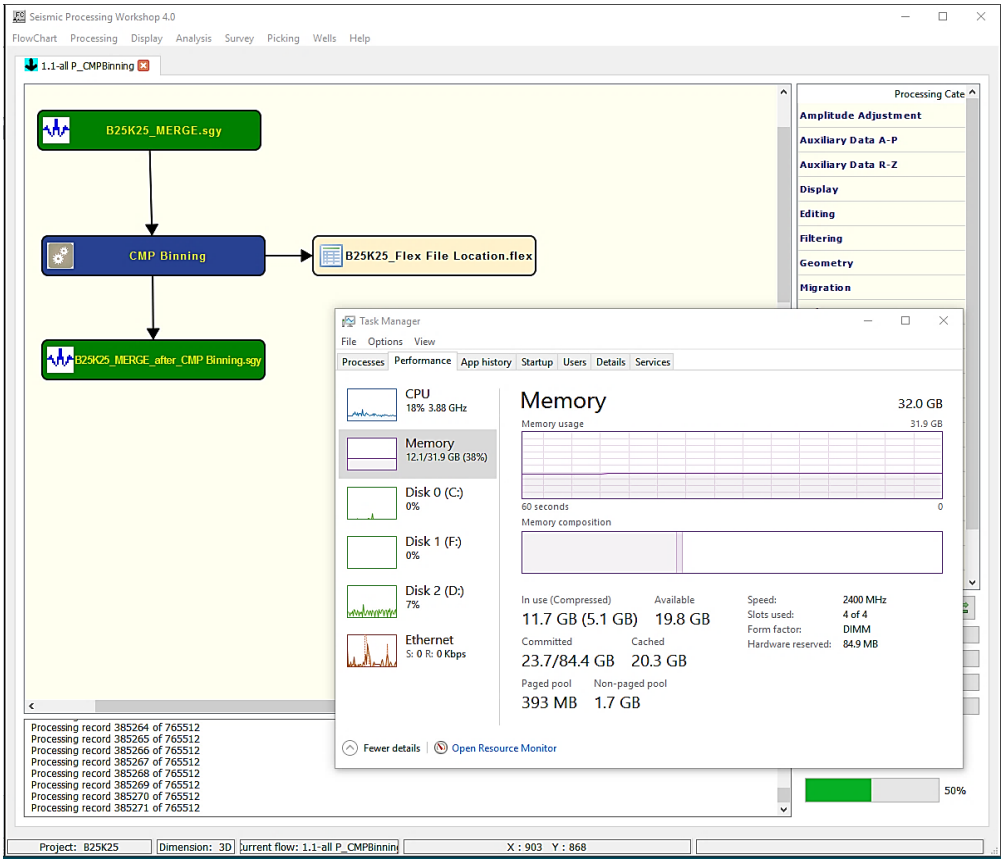

Figure 38. The memory used by computer, when ran the CMP *Binning* with the largest dataset of the survey area.

After fully testing and successfully solving all the problems associated with the CMP Binning Flex mode flow, a final test was carried out on the *Bin* Fold Limit flow. The trace selection method which was used in the CMP Fold Limit dialog box, was one trace per offset interval, which means assigning a trace to each *bin*, and not to have a regular fold. Some problems were detected in the *Bin* Fold Limit flow, with a set of error messages displayed:

"*** Error: Mismatch - First In-line on file is 1; *** Error: Mismatch - First Cross line on file is 17

*** Error: Cmp *Flex* Locations survey parameters do not match this data. Please remake the file.

*** Error: job initialization failed for process: *Bin* Fold Limit"

These *Bin* Fold Limit flow error messages are caused by the fact that the SPW team had to add some extra information to the *Flex* locations file to solve the issues detected during the execution of this work and these required changes in all subsequent flows. Also, at present, the *Bin* Fold Limit flow is also using too much memory while running (Figure 39), which also requires some extra *software* adjustments. More beta testing of this flow is now required.

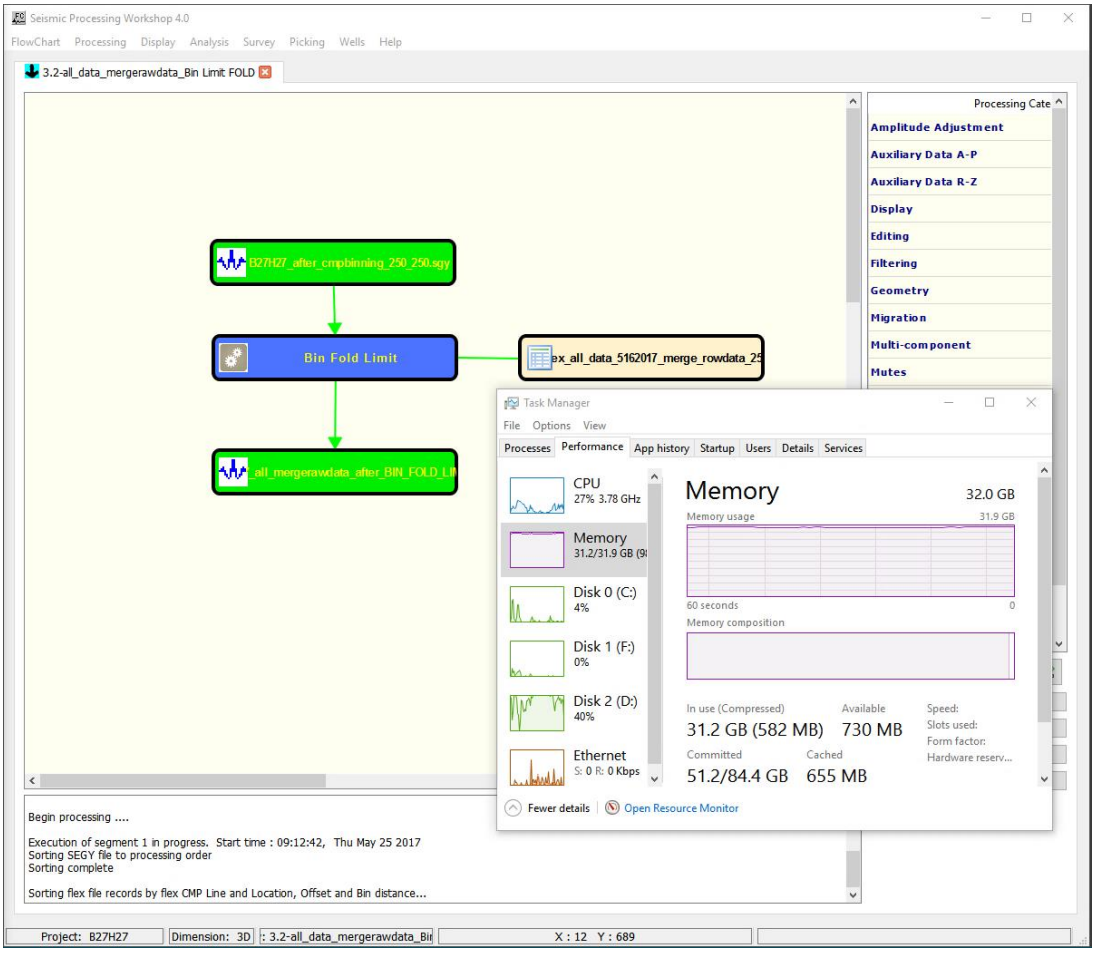

Figure 39. Memory usage when running the *Bin* Fold Limit flow with the Largest Size Dataset.

5. Results and Discussion

The *Flex Binning* routines, after all the tests performed and the resolution of detected bugs and code problems, is now working, which was one the main aims of this work. However, the *Bin* Fold Limit routine can still only be applied successfully to small datasets. For larger datasets, at present, the only solution is to cut them into small datasets, apply the *Flex Binning* by parts, and then merge the files, before performing the remaining processing steps.

In this Chapter, we show an example of the application of the *Flex Binning* to a portion of a 3D block from the study area, in which where the presence of data gaps is evident, to assess its performance.

5.1 Application of *Flex Binning* to a UHRS dataset

Next, we show an example of the application of the *Flex Binning* to a portion of a 3D block from the study area, in which where the presence of data gaps is evident (Figure 40). The bin size for this block is 1mx1m.

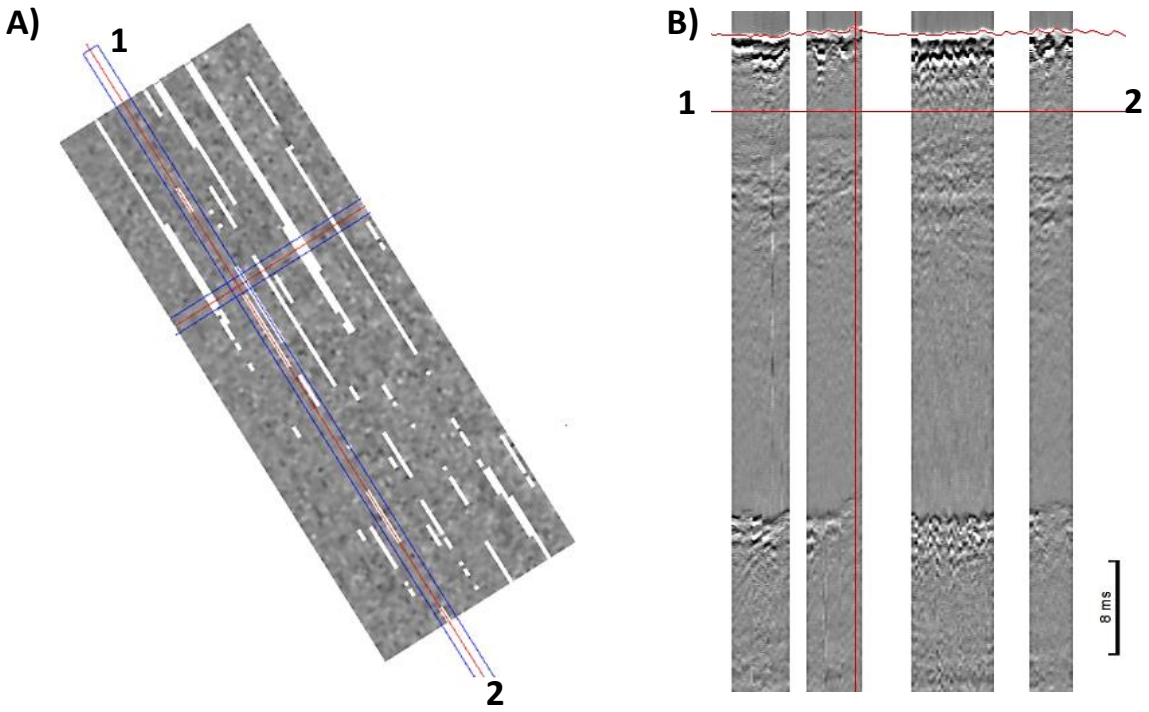

Figure 40. Example of a 3D block portion where the presence of data gaps is evident before the application of *Flex Binning*. A) Time slice display. B) Display of an ILine showing the data gaps.

This block was used to test *Flex Binning* with the aim to fill all the gaps which exist with the option of only one trace per *bin*. In order to get the images represented in Figure 41, Figure 42 and Figure 43 it was necessary to implement different % *bin Flex* for each seismic section. First, just to get an idea of the damage that can result when a too large flex percentage is used, a *Flex bin* percentage of 2000% (*Flex Bin* size of 21m x 21m) was assigned in both directions (crossline and inline). As can be observed in Figure 41, the result is not good. Overlap of many shots, leads to the distortion of the seismic data, causing a severe loss of resolution.

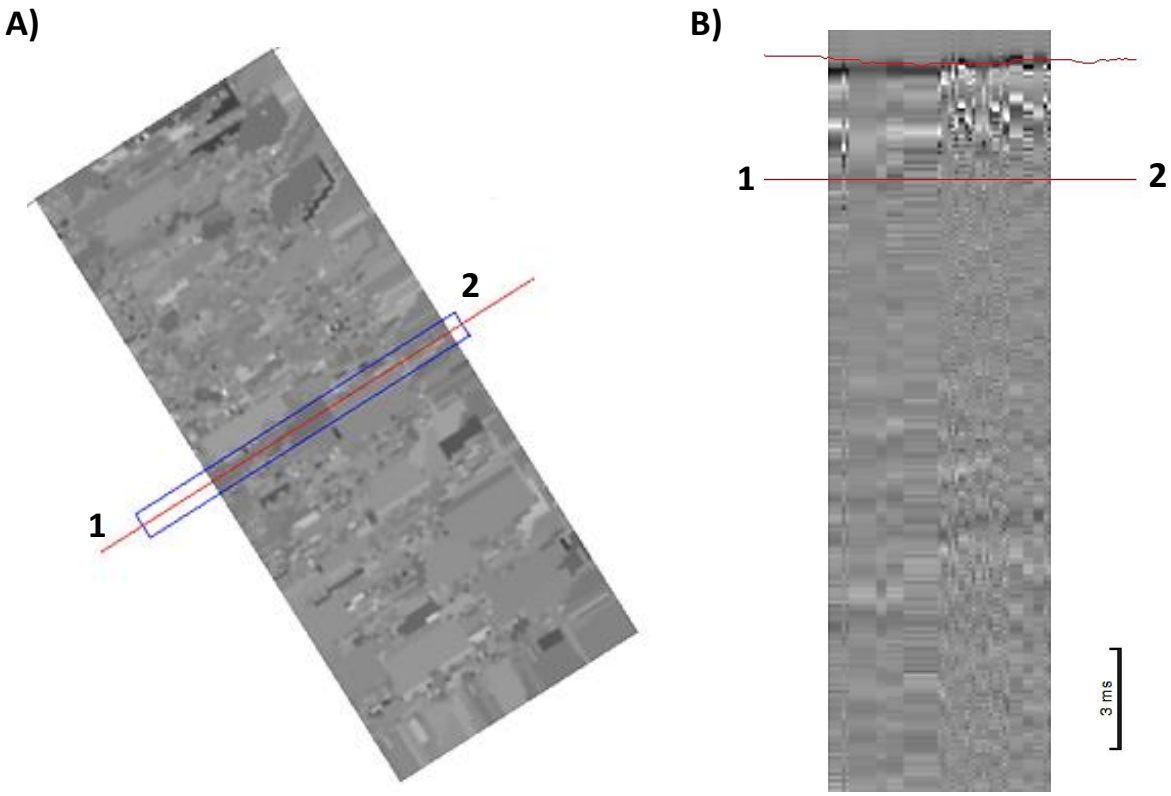

Figure 41. In this example, a *Bin Flex* of 2000% was assigned in both directions (crossline and inline) in a 3D block portion where is evident the presence of data gaps. A) Depth slice display. B) Display crossline. As can be observed there are no data gaps but there was a severe loss of resolution due to the choice of a too large Flex Bin percentage.

Next, a *Flex Binning* of 200% was used in both directions (Figure 42); this means that the *Flex Bin* size is now 3m x 3m, and therefore the new bin radius is 1.5m (see Figure 43). In this case, the *Flex Binning* fills in most of the gaps, but there still exist some gaps in the seismic data.

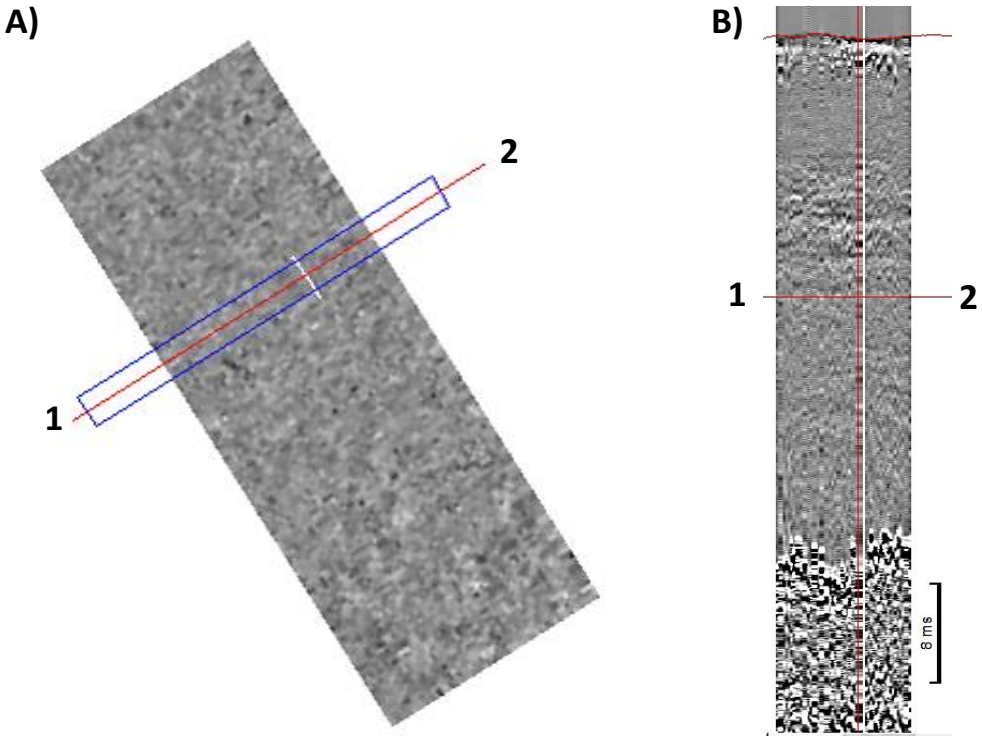

Figure 42. In this example, a *Flex* bin of 200% was assigned in both directions (crossline and inline) in a 3D block portion where the presence of data gaps is evident. A) Depth slice display. B) Display crossline.

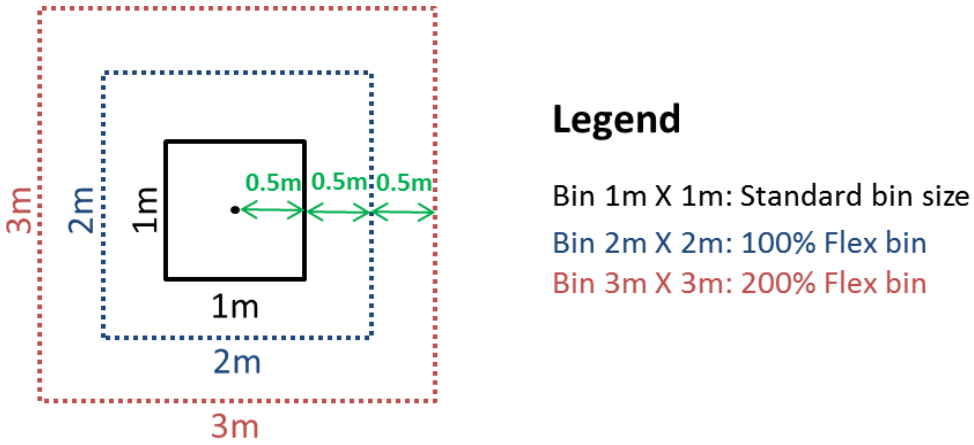

Figure 43. *Bin* expansion when *Flex Bin*nig is applied in SPW. Relation between bin radius and Percentage of Flex Bin.

Finally, a percentage *bin Flex* of 235 was used for both directions and the *Flex Binning* works very well, because it fills all the data gaps with an adequate seismic resolution (Figure 44). For a 235 % *bin Flex*, the *Flex Bin* size is 3.35m x 3.35m. In this case, the original bin radius of 0.5m increased to approximately 1.7m.

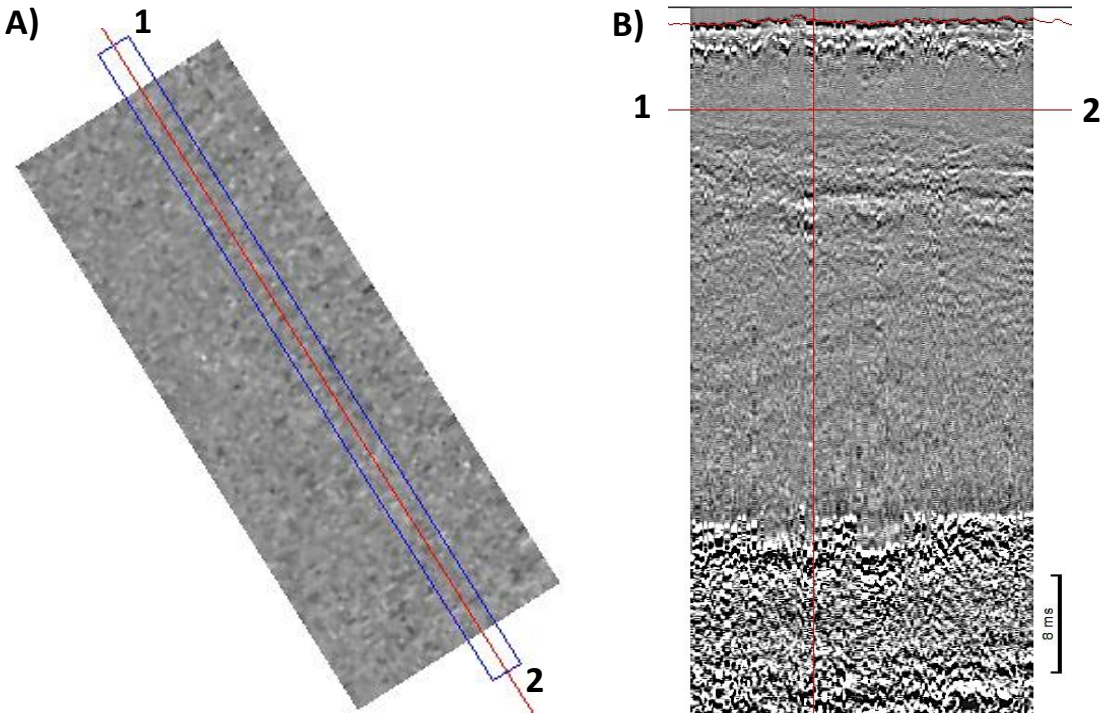

Figure 44. In this case, a *bin Flex* of 235% was assigned in both directions (crossline and inline) and excellent results were obtained. A) Depth slice display. B) Display inline.

5.2 Discussion

The challenge of the present work was to apply *Flex Binning* to very large ultra high resolution seismic (UHRS) datasets, in which the number of traces largely exceeded the available *software* design solutions and *hardware* capability. The implementation of an efficient and reliable *Flex Binning* to be applied to the data as soon as possible after data acquisition, if possible in the field, is a crucial step in industry as it will allow to assess the potential need or not to acquire new data before leaving the survey area. The SEG Y files used in the beta testing performed in the scope of this work contained more traces than the expected in a conventional seismic dataset, which highlighted *software* limitations, since SPW was not prepared for such data size. Besides the number of traces, there are at least 26 headers for each trace. This causes extra difficulties in the performance of the SPW, the computer *hardware* limits and time efficiency of processing.

Beta testing of the CMP *Binning* flow in different size datasets allowed code efficiency issues and *software* bugs to be detected, which allowed advances in the implementation of *Flex Binning* for large inputs, namely the successful execution the flow to a dataset with 751GB, which was a

major step forward. Before this work and tests, it was only possible to effectively apply *Flex Binning* to an input dataset with a size not greater than approximately 30 GB.

To successfully implement the CMP *Binning* step to a dataset with a substantial number of traces, one of the major issues was the inability to apply a grid to the dataset and leave traces out of the grid. The traces outside the specified area (grid) are now set as dead traces, and it is possible to flag those traces, so that the output seismic file does not include them.

Indexing was another issue which was solved by a change of *software* design in the CMP *Binning* code. The index problem consisted in the fact that the flow is running out of memory for the trace header list used to build the index file. The SPW team worked for to overcome this problem, creating an updated version of SPW which enables the index file to be created at the end of the processing, so that there will be a pause and scan of the data file before the ‘‘Processing Complete’’ message appears. This way, the SEG Y file is always completed and the index, which requires substantial memory, is created as a read after write operation on the output file, without the memory failures that were happening before due to the large dataset being processed.

Another critical issue that was solved concerns the memory usage in run time. In the first tests of the CMP *Binning* flow, the memory used by the computer was approximately 90%, but with the code improvement, now running the CMP *Binning* step with a large input only takes about 50% of the memory of the computer.

The time efficiency of processing is also very important. Beta testing allowed understanding how the processing time for different input files varies. The processing time can reach 22 hours, 26 minutes, 11 seconds for an input dataset with 751 GB, to get the *Flex* File Location card and the seismic output with the grid implemented.

Remaining issues to be solved include:

- The *Bin* Fold Limit flow adds *Flex* traces to the input binned data from an input *Flex* table. Due *software* design changes in the *Flex* Location File, the *Bin* Fold Limit flow does not yet work very well. This needs to be addressed.
- The map with the *Flex* location still does not work, because when we try to create the map from a *Flex* Locations File even with a relatively small dataset, some error messages still appear and SPW closes without any dump file. More testing on the *Bin* Fold Limit flow and generated *Flex* locations map is needed.

6. Conclusions

In general, the main objectives of this thesis were achieved. The main aim, which was to make the application of *Flex Binning* to large Ultra High Resolution Seismic Datasets a reality, by testing the existing *software*, detecting bugs and code issues and collaborating with the SPW development team on solving these issues, was completed. Finally, testing the application of the latest *Flex Binning* Flow to the largest dataset available in *Geosurveys* has proven a major step forward as it demonstrated the feasibility to use this method in the field just after data acquisition, which may save considerable time and money.

Gaps in 3D data cause highly adverse impacts in several steps of the data processing, making it impossible to obtain a final processed migrated volume. In the context of the implementation of Monopile foundations for offshore wind farms it is fundamental to be able to detect faults, boulders and other geological structures which represent a risk for the Monopile foundations implementation. Offshore wind farms are gaining popularity in the world and due to the current interest in the need for greener energy sources, security of energy supply and the public's reluctance to have wind farms on-shore. Efficient high resolution methods and quick ways to test the adequacy of the acquired data or the need to re-run parts of the survey as early as possible are fundamental.

The *Flex Binning* method is simple and fast when compared with alternative solutions (statistical interpolation and regularization) and therefore less expensive. The principle behind this step was used to correct navigation problems and feathering movements of the streamer during acquisition, because the *Flex Binning* can be a solution for irregular acquisition geometry.

Several tests were performed on the Seismic Processing Workshop *software* to accomplish the purpose of this work. Beta testing on CMP *Binning* flow allowed advances in the implementation of *Flex Binning* to large inputs, namely the execution this flow successfully to a dataset with 751GB. The Beta testing on SPW permitted to find problems in the code, and solve most of them. The issue of creating a map with the *Flex* location is already underway, but more work is still needed to solve it; and the same goes for the implementation of the *Bin* Fold Limit flow.

A good data *Flex Binning* is one which when applied to the dataset allows filling in the coverage gaps, without distorting the seismic data and without loss of resolution. The amounts of coverage gaps will influence the percentage which is to be used for the *Flex bin*. More data gaps require

larger flex percentages. High values of % *Flex bin* means that the search area will be also large. If the *Flex* trace search area is too large, then the greater the number of traces that are borrowed from neighboring *bins* and there will be significant amounts of traces to fill empty *bins* that may not to reliable estimates of the missing data. Due to this fact, the ability to distinguish seismic events can be lost, which leads to loss of seismic resolution making it impossible to detect small geological structures such as boulders, with potential risks for the Monopile foundations. Consequently, it is necessary to use common sense and care when using the *Flex Binning*, when the final product of seismic processing requires high seismic resolution.

In Future work, it is essential to continue to improve the code and beta testing of the CMP *Binning* flow, the *Bin* Fold Limit flow and generate fold maps from *Flex* File. The *bin* expansion in SPW should take the form of an ellipse in the future, where the shortest part is the direction of acquisition, thus allowing greater collection of traces.

The implementation of the *Flex Binning* in real-time during acquisition together with QC also in real time is now the goal for the future. This great advance will permit to reduce the infill/reruns made during the acquisition, to fill the gaps data, allowing to control the acquisition costs.

7. References

Amorim, D. N. (2014). *Caracterização de Reservatórios de Hidrocarbonetos do Bloco F3 do Mar do Norte.* Master Thesis: Department of Geosciences in University of Aveiro.

Anderson, B., & Borns, H. (1997). *The Ice Age World. Scandinavian University Press, 208 pp.*

Azevedo, L. (2009). *Seismic Attributes in Hydrocarbon Reservoirs Characterization.* Master Thesis: Department of Geosciences in University of Aveiro.

Balson, P., & Cameron, T. (1985). *Quaternary mapping offshore East Anglia.* Mod. Geol. 9, 221-239.

Balson, P., Butcher, A., Holmes, R., Johnson, H., Lewis, M., & Musson, R. (2001). *DTI Strategic Environmental Assessment Area 2, North Sea Geology.* British Geological Survey Technical Report, TR/008.

Besley, B. (1998). *Carboniferous In: Glennie, K.W. (editor) Petroleum geology of the North Sea, basic concepts and recent advances.* 4th edition: London, Blackwell Science Limited, 104-136.

Buia, M., Hill, D., Houbiers, M., Laura, S., Menlikli, C., Moldoveanu, N., & Snyder, E. (2008). *Shooting Seismic in Circles.* Oilfield Review, Autumn, 18 – 31.

Cameron, T. D., & Holmes, R. (1999). *The Continental Shelf. 125–139 in A revised correlation of Quaternary deposits in the British Isles. Bowen, D Q (editor). Special Report of the Geological Society of London, No. 23.*

Cameron, T. D., Stoker, M. S., & Long, D. (1987). *The history of Quaternary sedimentation in the UK sector of the North Sea Basin.* Journal of the Geological Society, London 144: 43-58.

Cameron, T., Crosby, A., Balson, P., Jeffery, D., Lott, G., Bulat, J., & Harrison, D. (1992). *United Kingdom offshore regional report: the geology of the southern North Sea.* HMSO, London.

Carr, S. J., Haflidason, H., & Sejrup, H. P. (2000). *Micromorphological evidence supporting Late Weichselian glaciation of the northern North Sea. Boreas 29: 315- 328.*

Caston, V. (1977). *A new isopachyte map of the Quaternary of the North Sea.* Institute of Geologist's Scientific Report 10/11, 3–10.

Collinson, J., Jones, C., Blackbourn, G., Besly, B., Archard, G., & McMahon, A. (1993). *Carboniferous depositional systems of the southern North Sea.* London: In: PARKER, J.R. (editor) Petroleum geology of Northwest Europe: proceedings of the 4th Conference, 677-687. The Geology Society.

Davies, B. J., Roberts, D. H., Bridgland, D. R., O'Cofaigh, C., & Riding, J. B. (2011). *Provenance and depositional environments of Quaternary sediments from the western North Sea Basin.* J. Quatern. Sci. 26, 59-75. .

Eisma, D., Mook, W., & Laban, C. (1981). *An early Holocene tidal flat in the Southern Bright. In Holocene, marine sedimentation in the North Sea Basin.* Special Publication of the

International Association of Sedimentologists (ed. X, Nio, R. T. E. Schuttenhelm & van Weering), vol.5 pp 229-237.

Ekman, S., & Scourse, J. (1993). *Early and Middle Pleistocene pollen stratigraphy from British Geological Survey borehole 81/26, Fladen Ground, central North Sea.* Review of Palaeobotany and Palynology, 79, 285–295.

Funnell, B. M. (1988). *Foraminifera in the Late Tertiary and Early Quaternary Crags of East Anglia. 50–52 in The Pilocene–Middle Pleistocene of East Anglia, field guide.*

GeoSurveys. (2016). *Standard operational procedure: Flex Binning using SPW.*

Glennie, K. W. (1986). *Development of northwest Europe's southern Permian gas basin. In: Brooks, J., Goff, J.C. and van Hoorn, B. (editors) Habitat of Palaeozoic gas in NW Europe.* London: Geological Society, Special Publication, 23, 3-22.

Glennie, K. W., & Underhill, J. R. (1998). *Origin, development and evolution of structural styles. In: Glennie, K.W. (editor) Petroleum geology of the North Sea, basic concepts and recent advances.* 4th edition: London, Blackwell Science Limited, 42-84.

Glennie, K., & Boegner, P. (1981). *Sole Pit Inversion tectonics. In: ILLING, L.V. and HOBSON, G.D. (editors) Petroleum geology of North-West Europe.* 110-120. London: Heyden and Sons.

Graham, A. G., Stoker, M. S., Lonergan, L., Bradwell, T., & Stewart, M. A. (2011). *The Pleistocene glaciations of the North Sea Basin.* In: Ehlers, J.; Gibbard, P.L.; Hughes, P.D., (eds.): Quaternary glaciations: extent and chronology: a closer look. Elsevier, 261-278.

Kearey, P., & Brooks, M. (1991). *An Introduction to Geophysical Exploration.* Blackwell Science, 2nd Edition.

Kearey, P., Brooks, M., & Hill, I. (2002). *An Introduction to Geophysical Exploration.* Blackwell Science 3rd Edition.

Kirby, G., & Swallow, P. (1987). *Tectonism and sedimentation in the Flamborough Head region of north-east England.* Proceedings of the Yorkshire Geological Society, 46, 301- 309.

Long, D., Laban, C., Streif, H., Cameron, T. D., Schuttenhelm, R. T., & Paepe, R. (1988). *The Sedimentary record and climatic variation in the southern North Sea.* Philosophical Transactions of the Royal Society of London, Series B, 318, 523-537.

McQuillin, R., Bacon, M., & Barclay, W. (1984). *An Introduction to Seismic Interpretation.* Graham d Trotman, 2nd Edition, 287 pp.

Plant, J. A., Whittaker, A., Demetriades, A., De Vivo, B., & Lexa, J. (2003). *The geological and tectonic framework of Europe.* Geochemical Atlas of Europe. Part, 1.

Reynolds, J. M. (1997). *An Introduction to Applied and Environmental Geophysics.* Willey, 796.

Ribeiro, A., Antunes, M., Ferreira, M., Rocha, R., Soares, A., Zbyzewski, G., . . . Monteiro, J. (1979). *Introduction à la géologie générale du Portugal, Serviços Geológicos de Portugal.* Lisboa: Internal. Géol. 26e, Paris, 1980, 114.p.

Ribeiro, T. D. (2011). *Multichannel Seismic Investigation of the Gran Burato area, off W Galicia.* Master Thesis: Department of Geosciences in University of Aveiro.

Sheriff, R. E. (2002 Fourth Edition). *Encyclopedic Dictionary of Applied Geophysics.* Society of Exploration Geophysicists.

Sheriff, R. E., & Geldart, L. P. (1995). *Exploration Seismology.* Cambridge university press. 2nd Ed.

Stoker, M. S., Balson, P. S., Long, D., & Tappin, D. R. (2011). *An overview of the lithostratigraphical framework for the Quaternary deposits on the United Kingdom continental.* British Geological Survey Research Report, RR/11/03. 48pp.

Telford, W. M., Geldart, L. P., & Sheriff, R. E. (1990). *Applied geophysics.* Vol.1 : 2nd ed. Cambridge university press.

Yilmaz, O. (2001). *Seismic Data Analysis: Processing, Inversion, and Interpretation of Seismic Data.* Society of Exploration Geophysicists, Volume 1.

Ziegler, P. A. (1975). *The Geological Evolution of the North Sea Area in the Tectonic Framework of North Western Europe.* Norges geol. Unders: 316 1-27.